Chapter 8
Evaluation of Geomechanical Properties of Soft Rock Masses by Laboratory and In Situ Testing

Luís Ribeiro e Sousa, Rita Leal e Sousa, Zhou Cuiying, and Karim Karam

8.1   Introduction

In recent years, the evaluation of geomechanical parameters in rock masses and particularly in soft rock masses has gone through significant improvements. This is partly due to improved measuring equipment and partly due to better numerical techniques. New instruments and equipment for in situ and laboratory tests allow for a more accurate evaluation of the properties of soft rock masses. Advancements in data mining (DM) techniques allow for better tools for decision making. The combination of improved instrumentation and more powerful numerical techniques allow for a better characterization of the geomechanical parameters of rock masses.

Due to the variability of rock formations, and the expense both in time and cost of obtaining subsurface information, there is a large degree of uncertainty associated with the evaluation of geotechnical properties. This is made even more uncertain given the complex geological processes involved and the inherent difficulties in geomechanical characterization (ASCE 1996; Sousa et al. 1997, 2010; Yufin et al. 2007; Miranda 2007; Miranda et al. 2009). As a result, the evaluation of geomechanical parameters is often carried out through in situ and laboratory tests along with the application of empirical methodologies (Bieniawski 1989; Barton 2000; Hoek 2007a, b; Miranda et al. 2018). For deformability characterization, in situ tests

L. R. e. Sousa (✉)
Tongj University, Shanghai, China

China University of Mining & Technology, Beijing, China

R. L. e. Sousa
Stevens Institute of Technology, Hoboken, New Jersey, USA

Z. Cuiying
Zhongshan University, Guanzhou, China

K. Karam
Sarooj Construction Company, Muscat, Oman

are normally carried out by applying a load in a certain way and measuring the corresponding deformations of the rock mass. For strength characterization, tests include shear and sliding tests which are often performed in low strength surfaces. These strength tests are expensive and strength parameters are often inferred indirectly by, for example, the Hoek and Brown (H-B) strength criteria normally associated with the GSI empirical system (Hoek 2007a; Hoek et al. 2008; Hoek and Marinos 2009). Laboratory tests are only relevant to a small rock volume and consequently it is necessary to perform a considerable number of tests in order to characterize the variability in geomechanical parameters, even if much effort is put in obtaining representative samples. Laboratory tests such as the determination of uniaxial compressive strength (UCS), point load and discontinuities tests are nonetheless important for empirical methodologies. Based on experience, it can be said that it is necessary to obtain direct geomechanical information from the site in study and it is insufficient to interpolate and extrapolate data from other sites.

Soft rocks exhibit unfavorable behavior related to low strength, high deformability, fast weathering, as well as others (Kanji 2014; He 2014). As such, sometimes testing equipment needs to be modified to accommodate for this. Soft rocks can be sedimentary rocks and weathered igneous and metamorphic rocks, or so-called residual rocks (Rocha 1975; Kanji 2014). The deformability moduli of soft rock masses, even those for residual formations can be considerably higher than those for soil formations. Lower bound of the deformability moduli of soft rock masses can be in the range of 0.4 GPa. For soils, lower values of cohesion can be in the range of 0.3 MPa, with friction angle of the same order of that for soft rocks (Rocha 1975).

For design purposes shear strength parameters are often selected rather than determined. The selection of deformability and strength parameters requires mainly sound engineering judgment, experience and on the use of empirical systems (ASCE 1996; Wyllie 1999; Sousa et al. 2010). The selection of design shear strength parameters in soft rocks is dependent on the particular site characteristics which include geological structures, planes of weakness, discontinuities, amongst others. In the soft rocks, discontinuities tend not to be as significant as for hard rocks. Failure envelopes for upper and lower bounds of shear strength can be determined for different types of potential failure surfaces, for example, in intact rock, with clean discontinuities and with filled discontinuities, and low strength surfaces. Technical Engineering and Design Guides issued by the US Army Corps of Engineers describe the appropriate selection procedures (ASCE 1996). Using the H-B (Hoek & Brown) criterion, Serrano and Olalla (2007) demonstrate the applicability of this criterion and the identification of applicable parameters based on the theory of plasticity. The rock mass is assumed to behave as a continuum and expressions are based in the theory of elasticity. Therefore, the selection of design parameters involves the selection of Poisson's ratio and deformability modulus. For almost all rock masses, Poisson's ratio varies between 0.1 and 0.35, and as a rule, lower values correspond to poorer quality rock masses. The selection of an adequate deformability modulus is important in order to make reliable predictions of deformations (Sousa et al. 2010).

Rock masses are in general described as heterogeneous and discontinuous media and their mechanical properties depend on both the rock material and the

discontinuity sets. In weak rock masses, the influence of discontinuities on the mechanical properties of the rock mass is not very significant. The evaluation of mechanical characteristics is influenced by the dimensions of the tested mass. In general, for deformability evaluation, the rock mass can be divided into zones, where each zone is considered as homogeneous based on its degree of weathering and discontinuity network. A reduced number of in situ large scale tests can then be performed in each zone. Small scale in situ tests in soft rocks should be performed in larger numbers for each zone. It is also important to perform laboratory tests for both deformability and strength in these type of rocks, and for the application of empirical systems, since the mechanical properties of the soft rock mass depend strongly of the properties of the rocks (Sousa et al. 1997).

The traditional empirical systems such as like RMR, Q and GSI systems (Bieniawski 1989; Barton 2000; Hoek 2007a; Kanji 2014) are also used in soft rocks. Strength is normally obtained by the H-B criterion using the GSI system (Hoek et al. 2005; Hoek 2007a). The use of the Q system is also recommended for the development of a new strength criterion (Barton 2013). There is, however some room for improvements to be made using artificial intelligence techniques, data mining (DM) techniques in particular. For example, a new empirical system was developed for heterogeneous volcanic rocks and validated using DM (Miranda et al. 2018).

Heterogeneities in rock masses are of great importance when evaluating mechanical properties of soft rocks, such as conglomerates, and residual rock masses. This is the case for the residual granite formations of Porto (Miranda et al. 2014), where the behavior of the rock mass is very unpredictable. As such, adequate measures need to be taken when planning and constructing engineering systems such as tunnels, for example continuous characterization of the tunnel face, real time monitoring to avoid accidents (Fig. 8.1), (Miranda 2007; Sousa et al. 2010; Sousa and Einstein 2012). A case study illustrating the characterization of a conglomerate for a fill dam in Japan will be presented in Sect. 8.2.4.

When dealing with rock masses, an important issue is the occurrence of surfaces with low strength. These can lead to significant consequences such as the accident
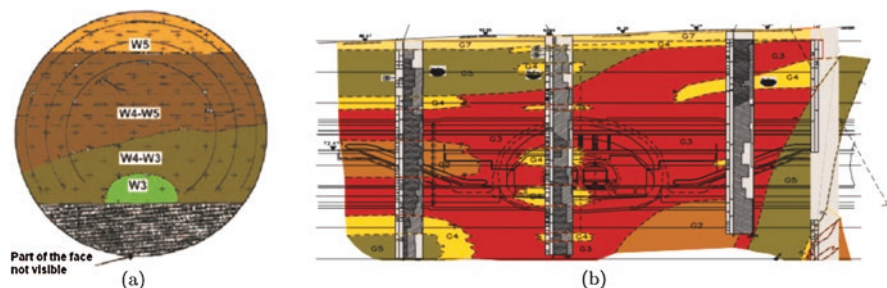
Fig. 8.1 Mixed face conditions found during the construction of the Metro do Porto: (**a**) View of a TBM tunnel face with different weathering degrees; (**b**) Cross-section of Bolhão underground station (Babendererde et al. 2006; Miranda et al. 2014)
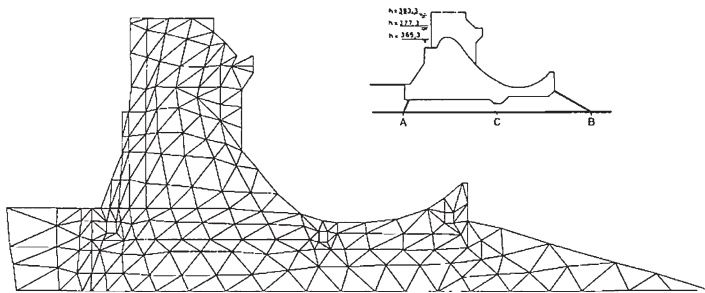
Fig. 8.2 Numerical model used for the study of Água Vermelha foundation. (Adapted from Pedro et al. 1975)
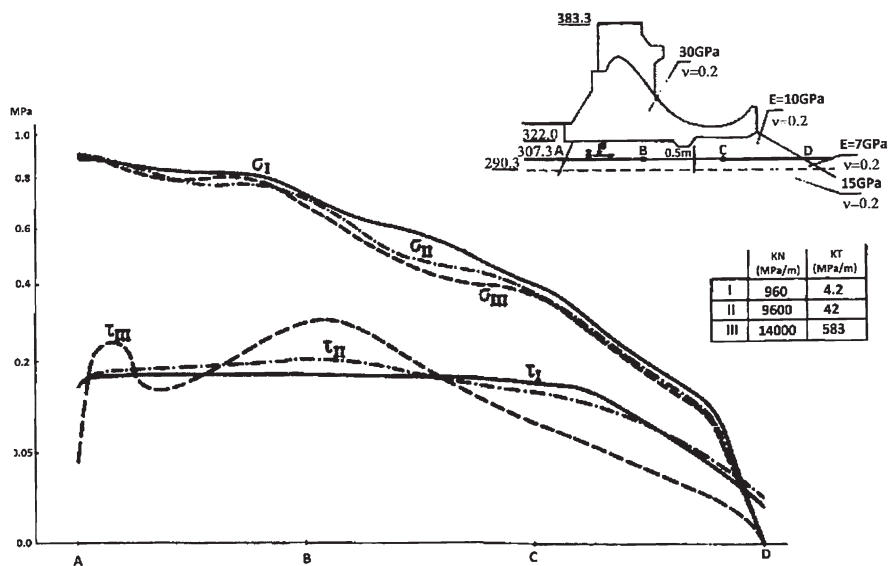

Fig. 8.3 Numerical results for the Água Vermelha foundation (Pedro et al. 1975; Rocha 1975)

that occurred during the construction of one of the surge chambers of the Cahora Bassa Hydroelectric Scheme in Mozambique (Rocha 1978; Sousa 2006, 2010).

Another case is that of the foundation of Água Vermelha dam in Brazil, in which an extensive basaltic circular sub-horizontal surface with thickness of 50 cm occurred (Pedro et al. 1975; Rocha 1975; Pacheco et al. 2017). Different finite element (FE) calculations were performed in order to analyze the structural behavior of the foundation for three hypotheses. Figure 8.2 shows the FE model used (Pedro et al. 1975). Results for the different hypotheses are illustrated in Fig. 8.3, assuming values for the normal and tangential stiffnesses KN and KT, respectively. The low strength surface was assumed to exhibit elastoplastic behavior with zero cohesion and a friction angle of 28°. Failure occurred in the extreme downstream zone for hypotheses I and II. The

distribution of tangential stresses tends to be uniform when the deformability of the low strength increases. It is possible to conclude that the risk of progressive rupture decreases with increasing deformability of the surface (Rocha 1975).

The chapter discusses in situ and laboratory tests used for deformability and strength evaluation and presents results in soft rock masses case studies. It is not the intention in this chapter to deal with all the laboratory and in situ tests for soft rock masses, but rather to establish a methodology to characterize the mechanical properties of these type of formations. Results of extensive testing on a very heterogeneous conglomerate rock mass at the site of a dam in Japan are presented.

8.2 Methodology for Evaluating Deformability

8.2.1 Deformability Evaluation

The evaluation of the deformability parameters of rock masses is essential for different applications in Civil and Mining Engineering. For many reasons, such as the heterogeneous and discontinuous nature of rock masses, anisotropy and others, the evaluation of the parameters is largely influenced by the dimensions of the tested volumes (Sousa et al. 1997; Rocha 1975, 2013).

The deformability characteristics of a rock mass can be determined by means of in situ and laboratory deformability tests, in which a load is applied in a specific manner, and the corresponding rock mass deformations are measured. To assess these characteristics, several types of tests are conducted on the rock and on discontinuities, which make it possible to obtain an acceptable representation of the rock mass behavior during and after the execution of projects. In some cases, rock masses are only homogeneous at very large scales and it becomes not economically feasible to perform representative tests. An insufficient test volume causes problems of scale effects (Rodrigues and Graça 1983; Simon and Deng 2009). The basic scale effects in deformability evaluation can be explained by the theory of statistics as follows (Grossmann 1993): whenever a rock mass deforms, the global deformation in a certain direction is the sum of a large number of small aleatory individual deformations in the same direction, of the different constitutive elements of the rock mass. Thus, from the laws of statistics, the global deformation has a normal distribution, whose mean value is independent of the number of summed individual deformations. Therefore, if the tests performed are chosen randomly, the experimental results should always present the same mean deformability and a standard deviation proportional to the square root of a significant length of the tested volume.

From these considerations, the deformability results obtained from small-scale tests are much more variable than those from large-scale tests. Thus, a sufficient number of tests should be performed in order to compensate for this variability. The tests for determining the deformability of rock masses must be performed prior to design. During construction, it is possible to obtain the response of the entire engi-

neering structure by monitoring and comparing the observed results with the predictions by numerical models. The reliability of the models depends fundamentally on the parameters that govern the behavior of the engineering system. Thus, it is important to use system identification techniques in order to re-evaluate the deformability parameters of the rock mass by taking into account the results obtained from monitoring and previous field tests (Castro and Sousa 1995).

Table 8.1 illustrates typical values for the deformability for soft rocks as well as shear strength values and UCS (Unconfined Compressive Strength). For low deformability rocks, deformability moduli can be considerably higher than those for soils. Table 8.2 shows the results of deformability moduli for soft rocks and corresponding rock mass values, for different types of formations in Spain, Angola, Taiwan, Greece, Iran, and Japan (Rocha 1975; Sousa et al. 1997; Hoek 2007a).

In the evaluation of deformability, it is important to consider anisotropy that exists in rock masses. In soft rock masses the anisotropy is mainly related with the rock anisotropy that influences the rock mass properties. Tests as shown in Table 8.2 were conducted parallel and normal to the schistosity. The relationship between tests perpendicular and parallel to schistosity varied between 0.3 and 0.9. In residual rocks, anisotropy also exists due to weathering effects (Rocha 1975). Therefore, deformability of soft rock masses should consider time effect (He et al. 2015b). Heterogeneity is also an important aspect to be considered, since all soft rock masses with low strength presents in general these characteristics. This is true for sedimentary rocks and for residual rock formations, which is the case for instance for a conglomerate formation from Yulin caves in China (Fig. 8.4) or for residual rock granite formations in Porto, Portugal (Fig. 8.5), (Medley 1994; Sousa et al. 2015).

Table 8.1 Deformability and strength range values for soft rocks (Rocha 1975)

Type of rock	E (GPa)	Shear strength		UCS (MPa)
		c (MPa)	φ (°)	
Claystone and siltstone				
Low	0.4–3.0	0.5–3.0	30–35	2–12
Average	3.0–8.0	3.0–6.0	35–40	12–25
High	8.0–30.0	6.0–12.0	40–55	25–80
Sandstone and conglomerates				
Low	0.5–4.0	0.5–3.0	30–40	2–12
Average	4.0–10.0	3.0–8.0	40–50	12–40
High	10.0–60.0	8.0–16.0	50–65	40–150
Limestones				
Clay	0.5–5.0	0.5–4.0	30–40	2–20
Shale	1.0–10.0	1.0–6.0	30–40	4–30
Sound	20.0–100.0	10.0–40.0	40–50	40–250
Schists				
Decomposed	0.4–2.0	0.4–2.0	30–35	1.5–8
Weathered	2.0–15.0	2.0–12.0	35–40	8–40
Sound	15.0–80.0	10.0–20.0	40–65	40–200

Table 8.2 Deformability in soft rocks and rock masses

Formation	Location	Region	E (GPa) Rock (E_r)	Rock mass (E_{RM})	$\alpha = E_{RM}/E_r$	Comments
Schist	Cedillo	Spain	90	40	0.44	Parallel to schistosity
Schist	Cedillo	Spain	40	12	0.30	Perpendicular to schistosity
Schist	Alcantara	Spain	140	5	0.04	Parallel to schistosity
Grés	Cambambe	Angola	65	8.6	0.13	Rocha (1964)
Conglomerate	Aviaki	Greece	60	6	0.10	Rocha (1964)
Siltito	Aviaki	Greece	15	1.5	0.10	Rocha (1964)
Argilito	Karum	Iran	11.5	7	0.61	Rocha (1964)
Limestone	Karum	Iran	50	7.5	0.15	Rocha (1964)
Sandstone	Mingtan	Taiwan	22.3	4.2	0.19	Perpendicular to schistosity
Sandstone	Mingtan	Taiwan	22.3	3.7	0.17	Parallel to schistosity
Siltstone	Mingtan	Taiwan	10.6	3.3	0.31	Perpendicular to schistosity
Silstone	Mingtan	Taiwan	10.6	5.7	0.56	Parallel to schistosity
Interbedded sandstone and siltstone	Mingtan	Taiwan	12.8	2.8	0.22	Perpendicular to schistosity
Interbedded sanstone and siltstone	Mingtan	Taiwan	12.8	3.0	0.23	Parallel to schistosity
Conglomerate	Site B	Japan	0.23	0.74	3.23	Sousa et al. (1997)
Conglomerate	Site C	Japan	0.22	0.50	2.27	Sousa et al. (1997)

For engineering purposes, it is useful to define a modulus reduction factor α, which represents the ratio of deformability modulus between rock mass and a smaller element of the rock material, as presented in Table 8.2. The two cases for conglomerates exhibit reduction factors greater than others due to the way the tests were performed in these heterogeneous formations.

Figure 8.6 represents the modulus reduction factor vs. the RMR coefficient. The correlation is based on values referred in the publication of Sousa et al. (2010). In accordance to the derived equation and considering that soft rocks can vary with RMR values between 40 and 10, the modulus reduction factor varies, respectively between 0.25 and 0.10, which can be considered in accordance to what is presented in Table 8.2.

In the following sections, in situ deformability tests are described which include borehole tests, plate load tests and flat jack tests, as well as laboratory triaxial tests including rockburst tests. A special reference is also made for the opening of galler-

**Fig. 8.4** Conglomerates at Yulin caves (Sousa et al. 2015)

Fig. 8.5 Geological cross-section of Bolhão station (Miranda et al. 2014)
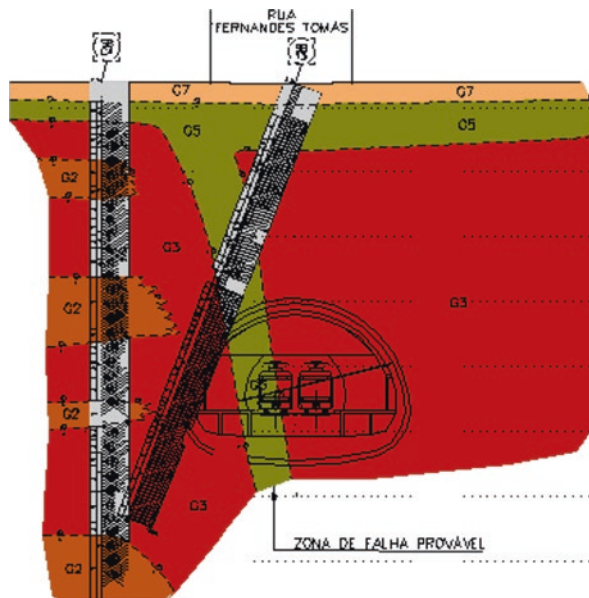
ies and in situ hydromechanical water loading tests. Sections are closed with rein-forced concrete plugs and measuring instruments are installed (Ulusay and Hudson 2007; Rocha 2013). A section is dedicated to a deformability investigation on a heterogeneous soft rock mass.

Fig. 8.6 Modulus reduction factor vs. RMR (Sousa et al. 2010)
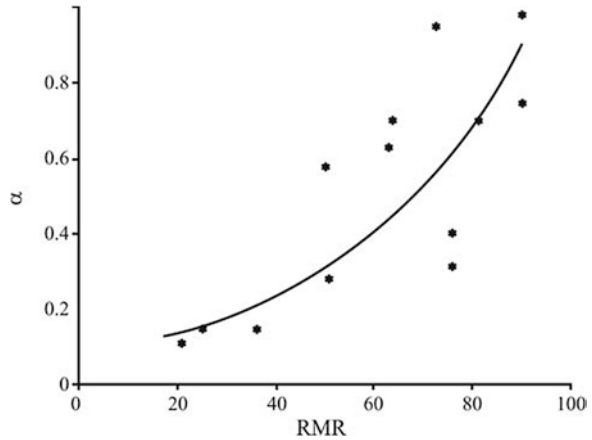
Table 8.3 Suggestions about the use of large scale tests for deformability evaluation

Situation	E (GPa)	Large scale tests
A	$E \geq 10$	Advisable
B	$5 \leq E < 10$	Necessary
C	$0.1 \leq E < 5$	Necessary with high precision

The general methodology, as mentioned in the Sect. 8.1, is to section the rock mass into different zones which are assumed homogenous (Graça 1983; Sousa et al. 1997). In each zone, several borehole tests can be performed to investigate the rock mass and deliver samples used for deformability tests, dilatometer or pressuremeter tests. The distribution of the tests can be of two distinct types: they can either be performed at random locations using a large number of tests in order to estimate mean values such as mean deformability; or they may be performed at in locations where the deformability modulus is expected to be lower (Sousa et al. 1997). To interpret the results, the criterion used for the location of the boreholes must be considered. In the case where a large number of tests are performed, there can be three distinct situations as shown in Table 8.3. For situation C, which corresponds to soft rock masses it is necessary to perform large-scale deformability tests with high precision, involving a representative test volume of the rock mass. In the same tested volume borehole tests should be performed, and the results obtained from both methods should be compared and correlated. With established correlations for each zone established, the results of other small scale borehole tests can then be corrected. Of course a large number of laboratory tests should be performed in each zone as they will be used for the application of empirical systems and also to compare with the in situ tests. The different types of deformability and strength tests, both in situ and in the laboratory, are described in Table 8.4.

Table 8.4 In situ and laboratory tests for deformability and strength (adapted from Sousa et al. 2010)

Purpose of tests	In situ tests	Laboratory tests
Deformability	Geophysical tests Dilatometer/pressuremeter LFJ and SFJ Borehole jacking Chamber pressure	Uniaxial compression Triaxial compression Swelling Creep
Strength	Direct shear Rock pressuremeter Uniaxial compression Borehole jacking	Uniaxial compression Direct shear Triaxial compression Direct tension Brazilian Point load

8.2.2   In Situ Deformability Tests

8.2.2.1   Borehole Tests

In situ deformability tests performed on a small volume are usually executed in boreholes, since the tests are relatively economical to be performed and in general the boreholes have already been drilled before in order to survey the rock mass. Moreover, preparation of the borehole walls in the test stretch is not required.

Borehole deformability tests can be grouped into the following two main types: (1) the pressure load is applied by means of a flexible membrane completely attached to the borehole walls with a rotationally symmetric pressure (referred to as dilatometers); and (2) the pressure load is applied by means of rigid plates attached to two arcs of the borehole's circumference (referred to as borehole jacks).

In the first type of test, rock pressuremeters are used to measure global volumetric deformation (Birid 2014, 2015). These tests are generally used for soil and weak rock and have accuracy limitations, because they measure volumes and not displacements. The use of rock pressuremeters for deep foundation design is very important, particularly for rock foundations in skyscrapers (Failmezger et al. 2005; Sousa et al. 2010). Other equipment is sometimes used and includes dilatometers with direct measuring devices in which several radial deformations can be obtained (Ulusay and Hudson 2007).

The second type of test corresponds to a more complex theoretical loading situation, such as in the case of the Goodman jack. The greater robustness of this equipment in comparison with the dilatometer is why it is still in use (Ulusay and Hudson 2007; Slope Indicator 2010), (Fig. 8.7).

The most suitable borehole tests for rock mass deformability characterization are dilatometer tests. The LNEC BHD (BoreHole Dilatometer) dilatometer is an old and reliable equipment (Graça 1983; Rocha 1974, 2013). It consists of a steel body, enveloped by a rubber jacket, which transmits pressure to the borehole walls. It was designed to carry out deformability tests for rock masses in NX (76 mm diameter) boreholes, operating under normal conditions up to 150 m deep (Fig. 8.8). The pressure
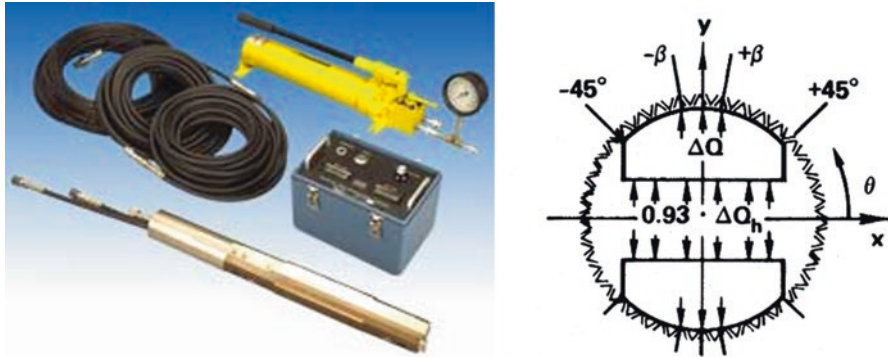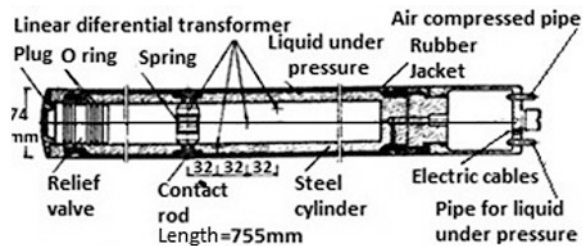
Fig. 8.7 Stiff dilatometer tests (Slope Indicator 2010)

Fig. 8.8 Borehole dilatometer BHD (Rocha 2013)

is obtained by pumping water, which can reach 20 MPa. The deformation is measured along four diameters, 45° apart, with the help of four pairs of sensors, which are connected to differential transducers. The deformability modulus, also called dilatometer modulus, is evaluated by assuming a continuous, homogeneous, isotropic and linear elastic medium, in accordance to the theory of elasticity for a borehole of infinite length with a uniform pressure acting on its wall (Graça 1983). These tests are easy to perform, but the tested volumes are small, usually between 0.5 and 1 m^3, and may not be representative of the rock mass. In soft rock masses, the results from dilatometer tests are more representative of rock mass behavior.

Other equipment is also available, such as the dilatometer probe presented by SolExperts (2016) and shown in Fig. 8.9. The specifications include measurements in depths up to 1400 m with borehole diameters of 96, 101, 122 and 146 mm, and maximum pressures up to 20 MPa (SolExperts 2016). Figure 8.10 shows a typical diagram pressure-deformation obtained in a point of a borehole.

Interpretation of these tests is difficult due to variations in the behavior of the rock mass during tests. In foundations, the initial stresses are small, and the tensile circumferential stresses induced by the applied pressure are usually higher than the initial circumferential stresses in the borehole walls. Thus, the deformability modulus obtained from the elasticity formula is not usually the true elastic modulus, but of an equivalent isotropic and homogeneous medium. Several assumptions can be made for the BHD dilatometer depending on the initial stresses (Pinto 1981; Sousa et al. 1997).

Fig. 8.9 Dilatometer
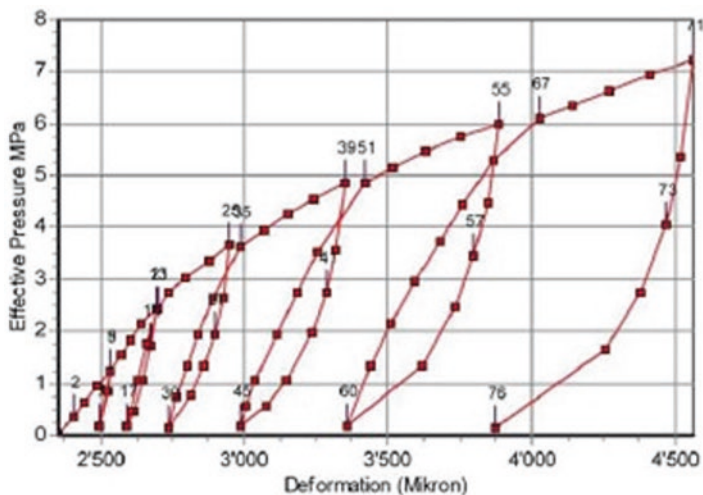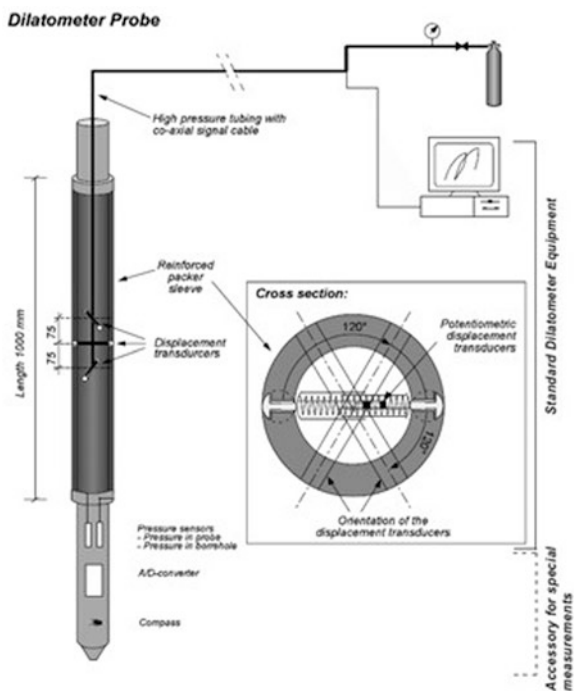probe SolExperts (2016)

Fig. 8.10 Diagram pressure vs. deformation in the dilatometer (SolExperts 2016)

   In soft rocks, it is necessary to have a rigorous characterization of the deform-
ability of the rock masses. In dilatometer tests results, the moduli of deformability
better represent reality. This is confirmed by the results in Fig. 8.11 where correla-
tions between the ratio of large deformability and dilatometer tests are correlated
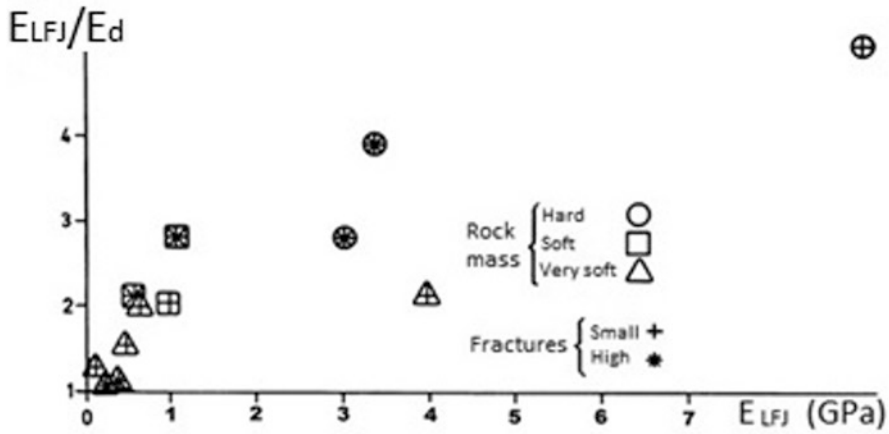
Fig. 8.11 Relationship between dilatometer deformability tests and large deformability tests (Graça 1983)

with the modulus of deformability of large deformability tests obtained by LFJ tests (Graça 1983). Figure 8.11 shows that the relation E_{LFJ}/E_{dil} can reach the value 5 for a rock mass with excellent quality, which can decrease to values near 1 for soft rock masses.

8.2.2.2 Plate Load Tests

In plate load tests (PLT), the load is applied on an existing surface and the response of the undisturbed rock mass is mixed with a superficial zone that is disturbed by the superficial stress release. To avoid this, sometimes only the deformation occurring at a certain distance from the load surface is measured, but measured deformations are usually smaller and therefore the results cannot be very accurate.

In situ PLTs should be based on a jack test (River Bureau 1986; Ulusay and Hudson 2007). The plate test using surficial loading is mainly performed in small tunnels or test adits. Two areas about 1 m in diameter are loaded using jacks. A typical test set up is shown in Fig. 8.12. Another scheme is shown in Fig. 8.13, for a double-plate bearing test with two hydraulic jacks applied to the walls of a gallery with a loading area of about 1 m^2 (Rocha 2013).

If the load is applied by a rigid-disk type plate to obtain a uniform displacement behavior, the modulus of deformability for the rock mass E_{MR} is given by Eq. (8.1):

$$E_{MR} = \frac{\left(1-\vartheta^2\right)\left(F_2 - F_1\right)}{2a\left(W_2 - W_1\right)}$$
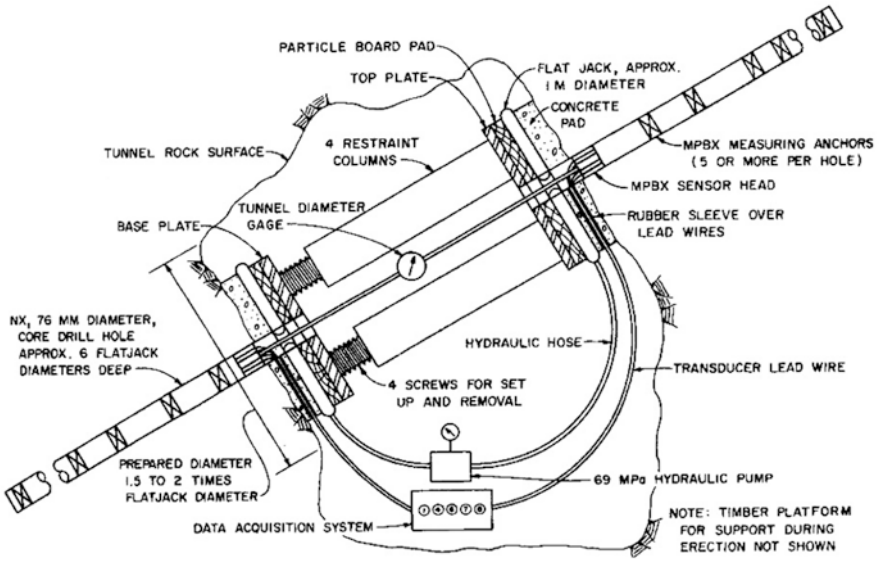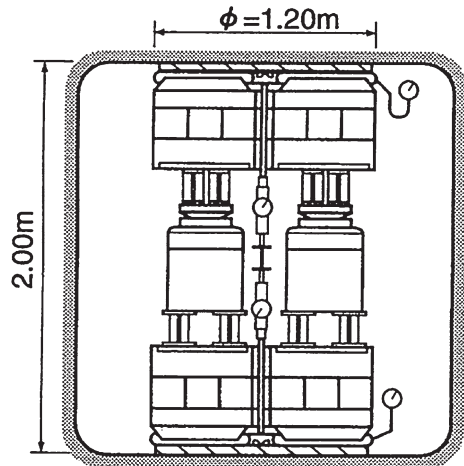
(8.1)

Fig. 8.12 Uniaxial jack test (Ulusay and Hudson 2007)

Fig. 8.13 Plate loading test arrangement used at LNEC (Sousa et al. 1997)

If the load is applied by a flexible flat-jack to obtain a uniform distribution load, E_{MR} is given by:

$$E_{MR} = \frac{2\left(1-\vartheta^2\right)\left(r_2 - r_1\right)\left(p_2 - p_1\right)}{W_2 - W_1}$$

(8.2)

In Eqs. (8.1) and (8.2), a is the radius of the rigid disk, ν Poisson ratio, F_1 and F_2 the loads of two points in the load vs. displacement curve, and W_1 and W_2 the displacement values corresponding to the pairs of forces and pressures F_1 and p_1, and F_2 and p_2, respectively.

There are indicated two types of PLTs as shown in Fig. 8.14. Two areas diametrically opposite in the test adit are loaded simultaneously, for example using flat jacks positioned across the test drift, and the rock displacements are measured in bore-
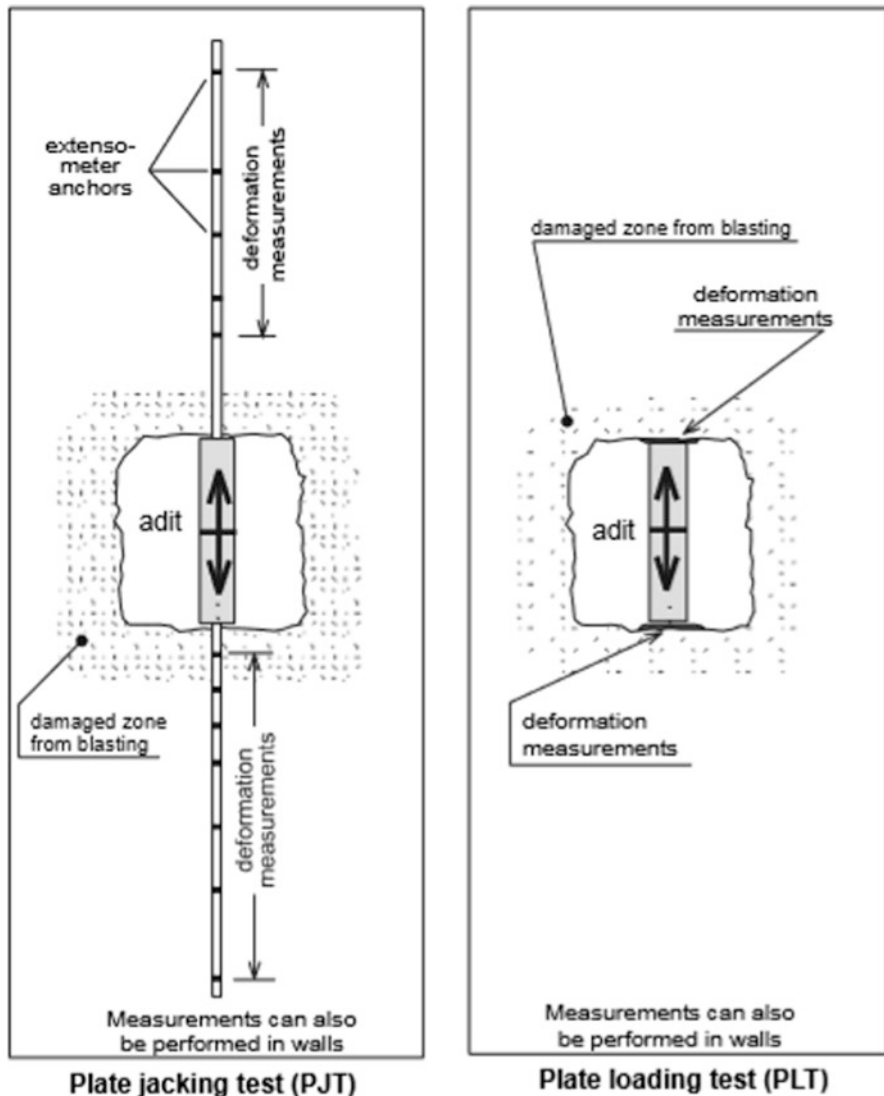

Fig. 8.14 Methods for PLT tests (Palmstrom and Singh 2001)

holes behind each loaded area (Palmstrom and Singh 2001). Alternatively (Fig. 8.14) the PLT measures the displacements at the loading surface of the rock, while the previous case records the displacements in drill holes beyond the loading assembly.

Mingtan Pump Station, in Taiwan

PLT tests were used at the Mingtan Pump Station, in Taiwan (Rodrigues et al. 1978; Hoek 2007a). The power cavern complex is located in sandstone, sandstone with siltstone interbeds and several siltstone beds belonging to the Waichecheng series. The sandstones are fine grained to conglomeratic and sometimes quarzitic. In general, they are strong to very strong although they are slightly to moderately weathered. Locally, softer zones of highly weathered material was encountered. The siltstones are moderately strong and almost always sheared. Occasionally, massive sandstone beds occurred with a thickness of up to 7 m. The geology of the Mingtan powerhouse is presented in Fig. 8.15. The general appearance of the rock mass in an exploration adit is shown in Fig. 8.16. Figure 8.17 shows the in situ PLT's.

Laboratory and in situ tests were carried out in the 1970s for the Mingtan Projects and the detailed design of the Mingtan project started in 1982 (Hoek 2007a). The rock mass in the powerhouse was classified using the RMR and Q systems as: Jointed sandstone—class 2; Bedded sandstone—class 3; Fault and shear zones— classes 4 and 5, as shown in Table 8.5. The in situ deformation modulus values for the rock mass are listed in Table 8.6.
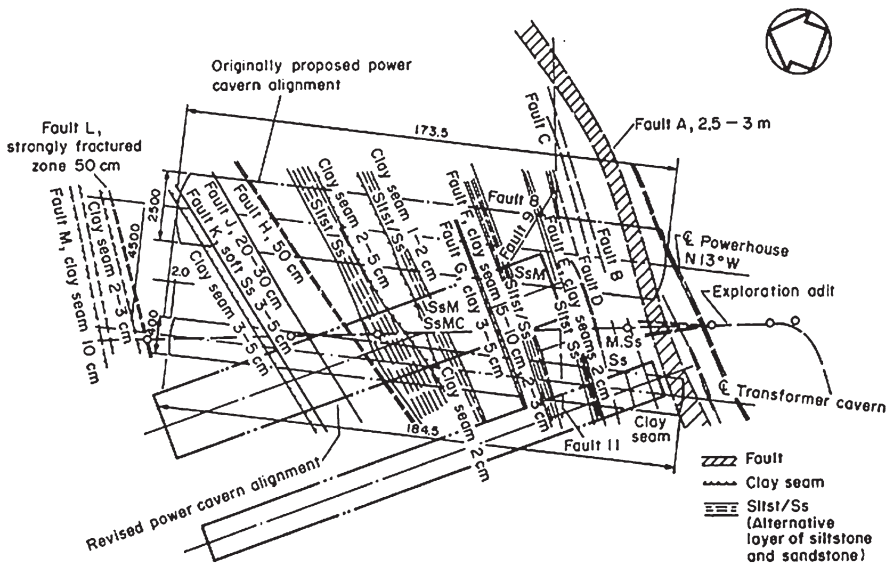

Fig. 8.15 Geological plan of the Mingtan underground powerhouse complex (Hoek 2007a)

Fig. 8.16 Sandstone and siltstone sequence in a adit (Hoek 2007a)

Fig. 8.17 Plate load tests
at New Tienlun
hydroelectric project
(Hoek 2007a)

Table 8.5 Rock mass classifications for the powerhouse area (Hoek 2007a)

Rock type	RMR	Q	Rock quality
Jointed sandstone	63–75	12–39	Good
Bedded sandstone	50–60	7–13	Fair to good
Fault and shear zones	10–33	0.1–11	Very poor to poor

Table 8.6 Deformation modulus of the rock mass from PLT tests

Rock type	Comments	PLT tests E (GPa)
Sandstone	Normal to bedding	3.2–5.1
	Parallel to bedding	2.3–5.0
Interbedded sandstone and silstone	Normal to bedding	2.8
	Parallel to bedding	3.0

8.2.2.3 Flat Jack Tests

In Large Flat Jack (LFJ) tests, a load is applied on the walls of a slot and the deformability of large volumes of rock masses in undisturbed conditions is assessed. The authors believe that LFJ tests are the most appropriate large scale tests for evaluating in situ the rock mass deformability. An LFJ test developed by LNEC is widely used by this institution in numerous studies in soft rocks (Pinto 1981). The advantage of this type of test in comparison with other slot tests is that the jacks can apply the pressure directly on the rock surface. The LNEC flat jacks contain four deformeters which measure the variation of the slot opening. The jacks can be placed in slots opened side by side and tested either simultaneously or individually, which allows one to conduct the test on a volume large enough to be representative of the rock mass. Figure 8.18 shows an arrangement of three flat jacks placed side by side.

The tests are usually interpreted using the Theory of Elasticity for a half-space, with a distributed normal load:

$$E_{LFJ} = \left(1 + v^2\right) K \frac{\Delta p}{\delta} \tag{8.3}$$

where E_{LFJ} is the deformability modulus obtained with these tests, ν is the Poisson ratio, K a constant to be evaluated, Δp the pressure change and δ the deformation caused by Δp. Constant K may be calculated by numerical methods and it is a function of the number of LFJ tests, the chosen deformeters and the depth of a crack that often develops in the plane of the slots during the tests (Pinto 1983; Rocha 2013).

An alternative LFJ arrangement is shown in Fig. 8.19 where in which each slot contains two independent jacks about half of the size of the old jacks and by a central borehole with 100 mm in diameter. The deformeters are placed in three independent measuring columns, installed in a central borehole and in two boreholes with 76 mm in diameter.
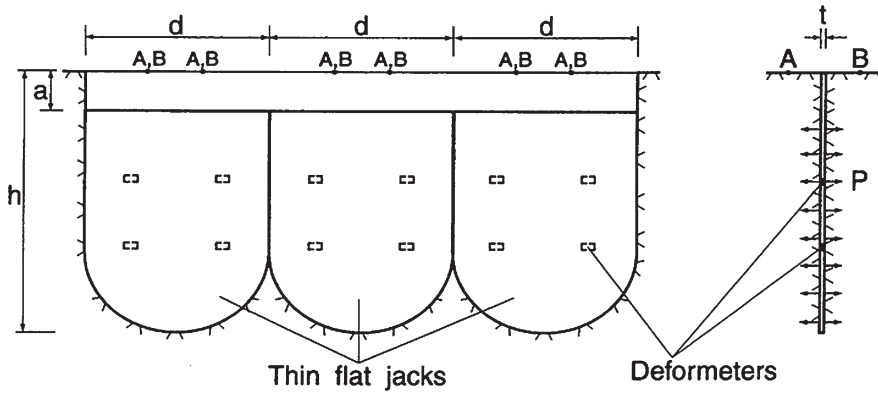
Fig. 8.18 Large flat arrangement with three slots

Fig. 8.19 New large flat jack setup (Sousa et al. 1997)
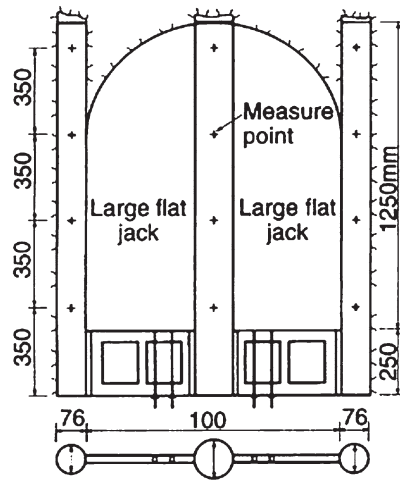
Another flat jack technique developed at LNEC is the Small Flat Jack (SFJ) using small scale jacks which are used mainly for stress measurements (Fig. 8.20), (Pinto and Graça 1983). However it can also be used to obtain the deformability of the rock mass assuming isotropic or anisotropic media (Martins and Sousa 1989). The following formula was obtained using results of a 3D finite element model (FEM):

$$E_{SFJ} = K \frac{\Delta p}{\delta} \tag{8.4}$$

Fig. 8.20 SFJ test. Geometry of a slot (Pinto and Graça 1983)

where E_{SFJ} is the deformability modulus, K a constant obtained through the FEM model, Δp the cancellation pressure and δ measured displacements between pairs of points.

An important application of the use of LFJ methods was at Mingtan Pumped Station, in Taiwan (Rodrigues et al. 1978; Hoek 2007a), presented in Sect. 8.2.2.2.

8.2.3 *Triaxial Techniques and Procedures in Laboratory*

High performance True Triaxial Testing (TTT) of rocks can simulate the in situ stress environment with three principal stresses with the goal to characterize the deformation and strength behavior of rocks. The state of the art of TTTs was discussed and reviewed during the Workshop on TTT of rocks held in Beijing (Kwasniewski et al. 2013). Some of the work has been published in Kwasniewski (2013), Lade (2013), Li et al. (2011), Mogi (2013), and Tshibangu and Descamps (2013).

In soft rocks Alexeev et al. (2013) presented experimental results of deformation and fracture of coals under true triaxial compression at various stress states. Lu et al. (2012) presented an experimental study of wellbore deformation in a deep claystone formation by using a large-scale physical true triaxial simulating equipment. Using cylindrical samples of Kimachi sandstone, Fujii et al. (2013) performed tests where confining pressures were applied through a liquid and the axial stress was applied by solid pistons as minimum principal stress. Tarasov (2012) demonstrated that hard rocks can exhibit dramatic embrittlement at a certain range of confining pressures, and proposes a special shear rupture to explain the phenomenon.

A special water–stress coupling meso-mechanics test system was developed at Zhongshan University, China (Zhou 2018). It uses conventional rock triaxial appa-

ratus with oil to provide confining pressure and requires that the rock sample be protected by an envelope. In practice, it is very difficult to simulate softening conditions of soft rock (taking into account water-stress coupling), and it is difficult cannot meet the requirements of observing meso-characteristics on the surface of soft rock under water-stress coupling. This was the motivation to develop the apparatus to simulate the deformation of and failure process of soft rock in the real environment. The so-called "TAW-100 water-stress coupling soft rock meso-mechanics servo triaxial test system" was created improving the loading system, pressure chamber and microscopic observation part of traditional rock triaxial testing machines (Zhou 2018). The design of the new system is shown in Fig. 8.21, where A is the pressure chamber; B is the loading system; C is the measuring system; D is the servo control system; E is the microscopic observation system; F is the computer system; G are the rock samples. The loading system consists of an axial pressure system and a two-direction confining pressure servo loading system. The system can adjust the axial pressure and radial confining pressure on rock samples with different time intervals according to different experimental programs in order to make it possible to simulate the pressure situations for soft rock under various construction programs, and provide the function of filling and compressing the pressure chamber with water or oil. The axial loading system is illustrated in Fig. 8.22. The two-direction confining pressure servo-loading system is presented in Fig. 8.23. It consists of a rigid support, ball screw, servo-motor, water and oil reservoirs, piston hydraulic sensor, etc.

More details of this equipment can be found in the report of Zhou (2018).

A modified true triaxial test system to for TTT of rocks was developed at SKL-GDUE, of the China University of Mining and Technology, of Beijing (He et al. 2013) and is shown in Fig. 8.24. This innovative equipment has a single face unload-
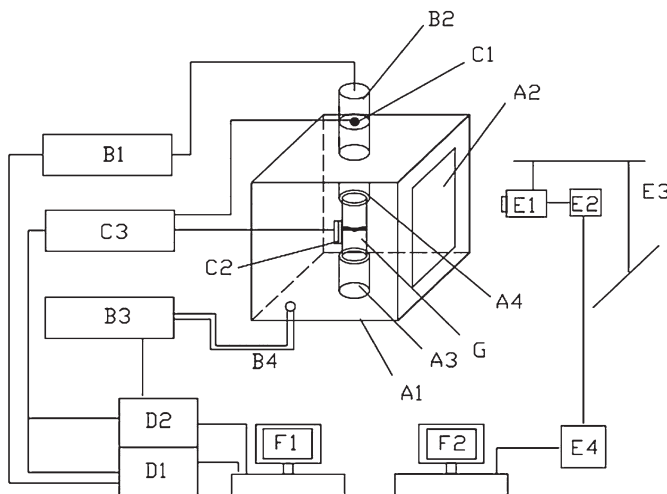
Fig. 8.21 Design of a new test system

**Fig. 8.22** Axial pressure
loading system

ing device that allow one to perform rockburst tests in laboratory (He and Sousa
2014; He et al. 2015a). Figure 8.25 describes the dropping test used for unloading a
face which is performed through a change of a piston movement.

Since its development, a large number of rockburst tests were performed and the
results of the tests collected, and stored in a database which was analyzed. This
included studies from several countries including China, Italy, Canada and Iran.
DM techniques were applied and predictive models were developed for the rock-
burst maximum stress (σ_{RB}) and for a rockburst risk index (I_{RB}). All the tests were of
strainburst type. A rockburst critical H_e was calculated by the following expression:

$$H_e = 18.52\sigma_{RB} \tag{8.5}$$

where σ_{RB} is the rockburst maximum stress obtained in the test and H the depth
where the sample was collected. The index I_{RB} was proposed and calculated from
the formula (He et al. 2015a):

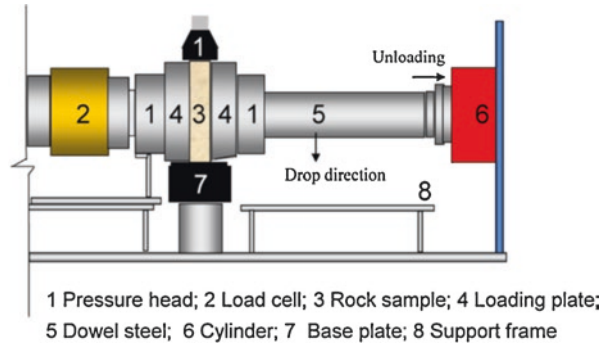$$I_{RB} = \frac{H}{H_e} = 0.054\frac{H}{\sigma_{RB}} \tag{8.6}$$
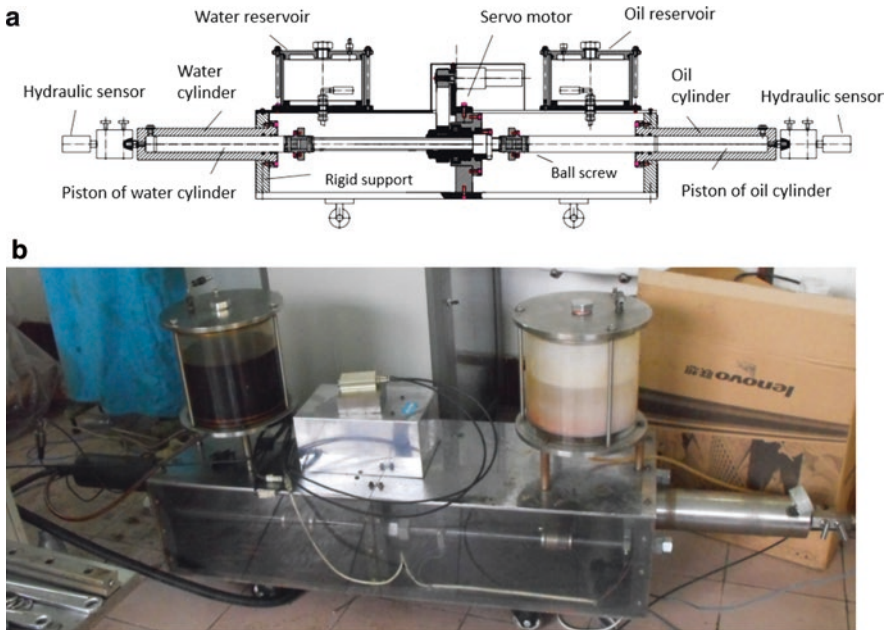
Fig. 8.23 Two-direction servo confining pressure loading system. (**a**) Design diagram of two-direction servo confining pressure loading system. (**b**) Photo of two-direction servo confining pressure loading system physical
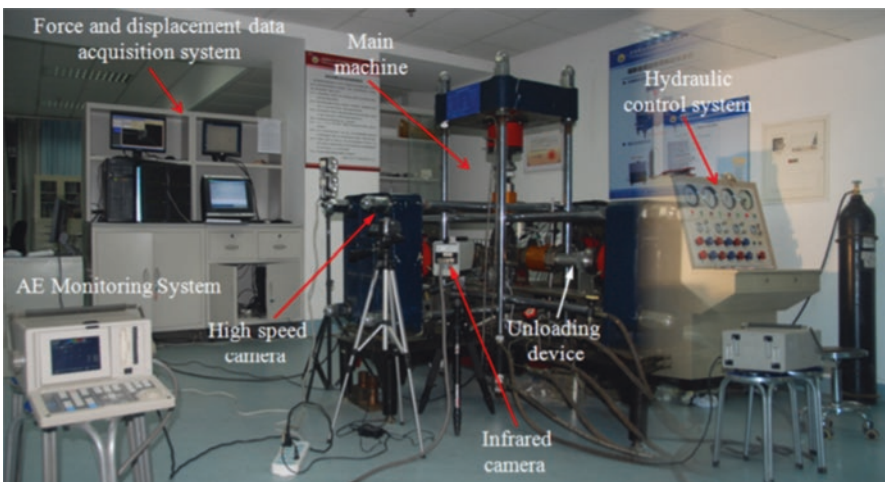
Fig. 8.24 Rockburst testing system (He 2006)

Fig. 8.25 Illustration of the dropping system for load bar and loading plate (He 2006)

1 Pressure head; 2 Load cell; 3 Rock sample; 4 Loading plate; 5 Dowel steel; 6 Cylinder; 7 Base plate; 8 Support frame

Table 8.7 Statistical parameter values of soft rocks obtained through rockburst tests

Parameters	Schist	Coal	Dolomite	Limestone	Mudstone	Sandstone	Shale	Slate
UCS (MPa)	–	11.9	–	24.1	11.5	83.4	8.0	58.3
E (GPa)	–	2.4	–	9.7	2.0	24.5	3.0	13.5
ν	–	0.28	–	0.24	0.37	0.24	0.37	–
H (m)	1000	507	250	3375	910	854	500	500
H_e (m)	1413	352	2315	1278	306	1878	343	1587
σ_{RB} (MPa)	76.3	19.0	125.0	69.0	16.5	101.4	18.5	85.7
I_{RB}	0.81	1.65	1.11	3.49	3.02	0.62	1.54	0.34

Some of most important statistical characteristics concerning the database are presented in Table 8.7 for soft rocks (schist, coal, dolomite, limestone, mudstone, sandstone, shale, and slate). The DM models made it possible to predict the parameters in Table 8.7 with high accuracy using data from the rock mass and a specific project. The DM modeling techniques comprised MR—Multiple Regression, ANN—Artificial Neural Networks, and SVM—Support Vector Machines.

A classification in accordance with the rockburst index was established for the possibility of occurrence of rockburst depending on the value of I_{RB}. For $I_{RB} < 0.6$ is classified as Low; $0.6 < I_{RB} \leq 1.2$ is classified as Moderate; $1.2 < I_{RB} \leq 2.0$ is classified as High; and $I_{RB} > 2.0$ is classified as Very High. Figure 8.26 shows the relation between I_{RB} and σ_{RB}.

Among the DM algorithms used only MR provides an equation relating the output and the input variables. The modeling and evaluation is discussed in He et al. (2015a). The equations are:

$$\sigma_{RB} = 9.132 - 0.013H + 0.381UCS + 0.364E + 1.211\sigma_{h1} - 0.069\sigma_{h2} + 0.365\sigma_V \quad (8.7)$$

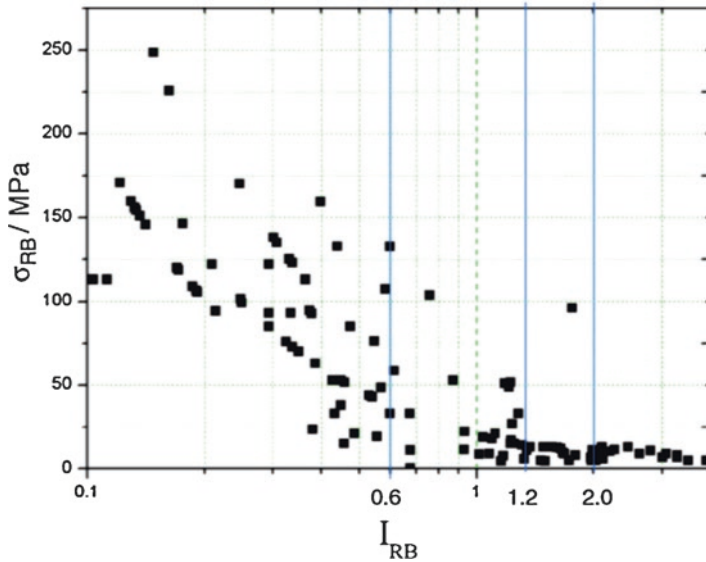$$I_{RB} = 1.432 + 8.035\,10^{-4}H - 8.429\,10^{-4}UCS - 0.009E - 0.007\sigma_{RB} - 0.074K \quad (8.8)$$

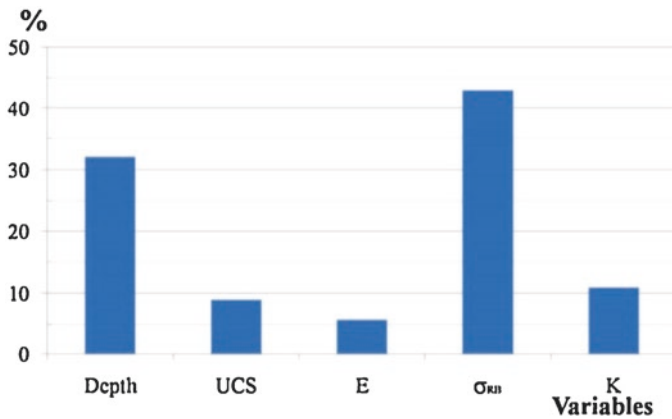**Fig. 8.26**   Distribution of I_{RB} vs. σ_{RB} (He et al. 2015a)

Fig. 8.27   Importance of variables for predicting I_{RB} using ANN model (He et al. 2015a)

In Eqs. (8.7) and (8.8), σ_{h1} and σ_{h2} are, respectively, the horizontal in situ stresses in a perpendicular and in the face to be unloaded, and K is ratio between the average in situ horizontal stresses and the in situ vertical stress due to overburden. Figure 8.27 shows the relative importance of the variables for predicting I_{RB} in the more accurate ANN model.

**Fig. 8.28** Galleries TA-3 and TA-3′. Location of the tests
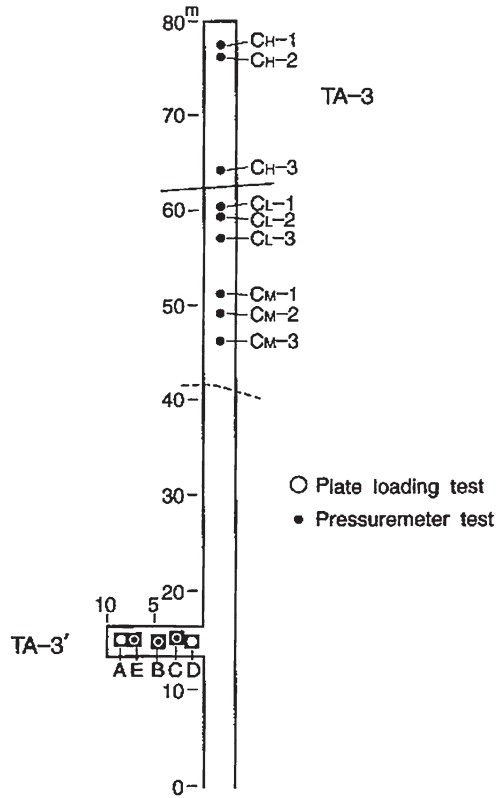
8.2.4 Deformability Investigation of Soft Rock Mass at a Dam Site in Japan

In this section the evaluation of the deformability parameters is discussed in the context of the foundations of a dam in the north of Japan (Sousa et al. 1997). The rock mass is highly heterogeneous and consisted of lapilli tuff and conglomerates.

A main gallery about 80 m long was excavated as shown in Fig. 8.28, and several in situ and laboratory tests were performed on rock samples. In situ PLTs were performed on a small gallery designated TA-3′ perpendicular to the main gallery (Fig. 8.29). The PLTs were performed considering rigid plates with 30 and 60 cm in diameter, mainly in the conglomerate formation. Nine in situ pressuremeter tests were performed in the locations indicated in Fig. 8.28, namely C_H-1, C_H-2, C_H-3, C_L-1, C_L-2, C_L-3, C_M-1, C_M-2, and C_M-3. Some laboratory tests were carried out that included uniaxial compression tests and measurement of the velocities of waves and specific gravity.

PLT tests were performed at five locations in the gallery TA3′ designated by A (No. 1), B (No. 2), C (No. 3), D (No. 3′), and E (No. 4). The loading tests were

Fig. 8.29 Detail of the location of plate load tests at the gallery TA-3′
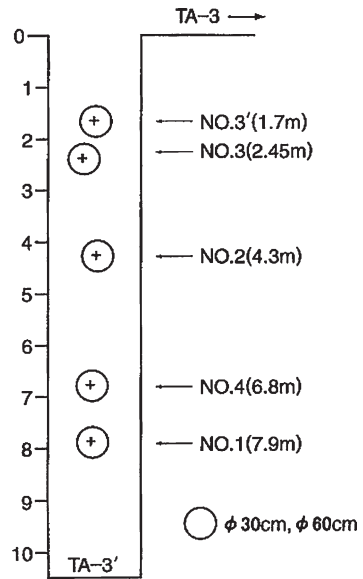
Fig. 8.30 Loading pattern for the plate load tests
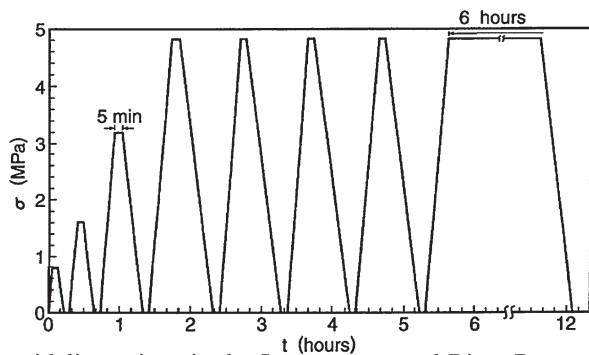
performed according to the guidelines given in the Japanese manual River Bureau (1986). The loading pattern was based on four incremental steps of 0.8, 1.6, 3.2, and 4.8 MPa for four cycles repeated for the last increment of load as indicated in Fig. 8.30. A final endurance loading cycle was carried out for 6 h. The coefficient of deformation D, tangential coefficient E_t and secant coefficient of elasticity E_s were determined in accordance with the example of load-displacement curves presented in Fig. 8.31.

Figure 8.32 is a schematic of the bedrock observed in the exploratory TA-3′, which was excavated along the right bank of a river in the conglomerate layer (Sousa et al. 1997). The conglomerate is pale dun-greenish dun and its heterogeneous bedrock consists of gravel and matrix. The bottom of the exploratory gallery is relatively dry and the ground water level was about 40–80 cm below the bottom. The gravel is made up of lapilli tuff, coarse-grained tuff and mudstone. The main gravel size ranged from 5 to 50 cm, but large gravel measuring 2 m in size was
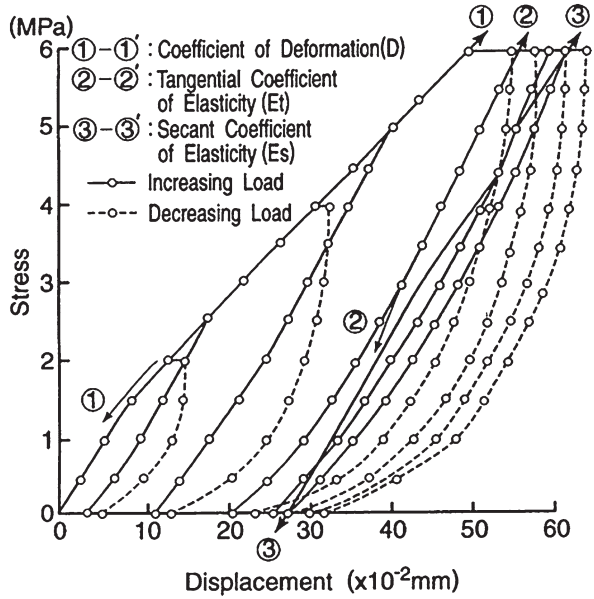
Fig. 8.31 Example of load
vs. displacement curves

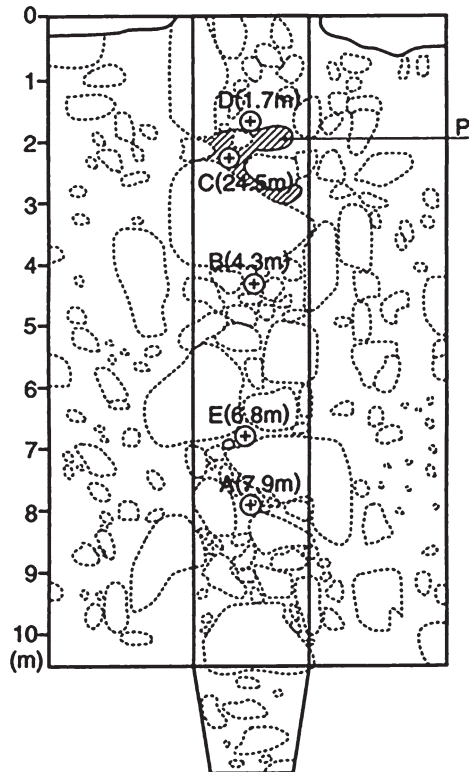**Fig. 8.32** Heterogeneity
involved by PLT tests
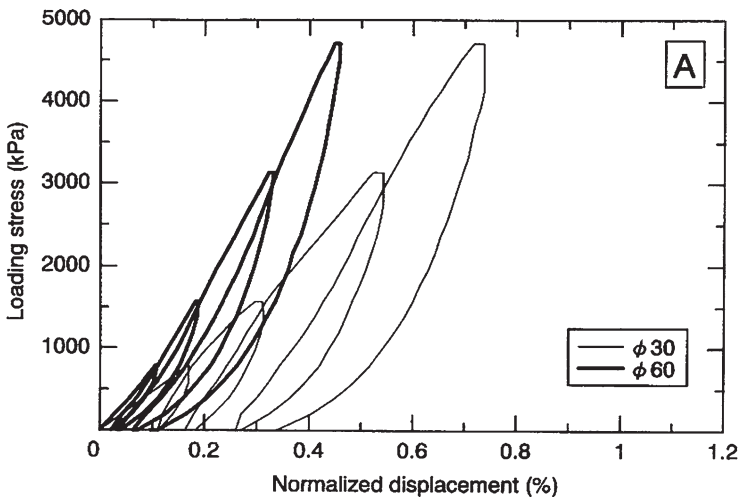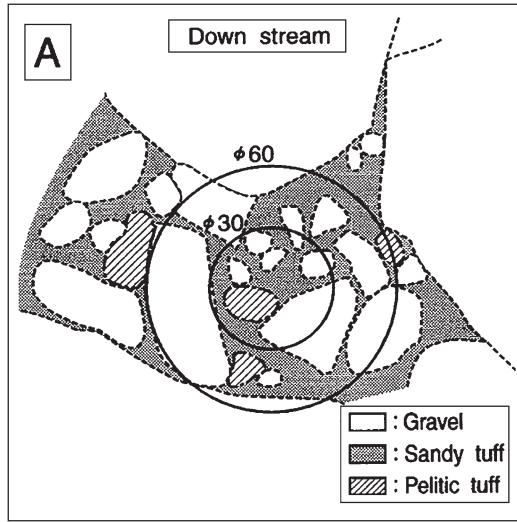
Fig. 8.33 Sketch of the test surface A

Fig. 8.34 Diagram of loading stress vs. displacement for the PLT tests at A

found in places. The matrix is soft and consisted of sandy tuff and politic tuff, and has a low degree of consolidation.

The test site consists of gravel of various sizes and a small-scale matrix that lies in between. A detailed sketch of the rock formation in the location was made for each site location. Figure 8.33 presents a detailed sketch for the test surface A. In each test site a PLT with 30 cm diameter was first performed, followed by a PLT with 60 cm diameter. The tests were performed in areas where the matrix and gravel were in an approximate equal proportion.

Figure 8.34 shows typical results for the relationship between loading stresses and displacements at site A. The normalized displacements represent the average

Table 8.8 PLT test results

Position	30 cm plate			60 cm plate		
	D (MPa)	E_t (MPa)	E_s (MPa)	D (MPa)	E_t (MPa)	E_s (MPa)
A	578	1014	818	886	1307	906
B	413	808	639	736	1159	789
C	47	439	410	487	953	641
D	634	1119	852	914	1413	931
E	736	1225	1019	1243	1667	1511

Table 8.9 Pressuremeter test results

Test	Class	D (MPa)	E_t (MPa)
C_L-1	C_L	30	210
C_L-2	C_L	350	890
C_L-3	C_L	60	300
C_M-1	C_M	1260	1890
C_M-2	C_M	2160	6900
C_M-3	C_M	1730	2770
C_H-1	C_H	1870	13,000
C_H-2	C_H	2890	5200
C_H-3	C_H	2590	8650
B	C_L	220	1240
C	C_L	130	540
E	C_L	690	1200

values of the four points on the stiff plate as a percentage, obtained by dividing the displacements by the diameter of the plate. The results show that the slope of the tangent of the curves increases as displacements of the plate increases, which means that the rock formation gets harder with increasing stresses.

Tests conducted at another site, C, showed extremely large deformations for the PLT's with 30 cm diameter, but the PLT with diameter 60 cm did not show such large deformations. This happened because the plate probably was on the matrix, where the gravel area ratio is different to the other tests.

Table 8.8 summarizes the PLT results. In order to calculate the coefficient of deformability D, the range of loading stress was from 2 MPa (test B), to 2.2 MPa (tests C, D and E), to 2.4 MPa (test A) to 4.8 MPa (for all tests). E_t was calculated for a lower pressure between 1.0 and 2.8 MPa and for a higher stress between 4.0 and 4.8 MPa. E_s was determined for the range of stresses between 0 and 4.8 MPa.

Several pressuremeter tests were carried out for a 66 mm diameter borehole. Six tests were performed on lapilli tuff (classes CM and CH) in gallery TA-3′ and six in the conglomerate rock mass, three being in the same location of plate load tests B, C and E as indicated in Fig. 8.28. Three additional tests were performed in class CL in TA-3. Some results are shown in Table 8.9.

Several laboratory tests were performed in order to evaluate the deformability modulus and the uniaxial compressive strength (Sousa et al. 1997). A summary of

Table 8.10 Deformability moduli at a heterogeneous conglomerate for different tests

| Test	Deformation coefficients	Maximum (MPa)	Mean (MPa)	Minimum (MPa)
PLT (60 cm)	D	1243	853	487
	E_t	1667	1300	953
PLT (30 cm)	D	736	482	47
	E_t	1225	939	439
Pressuremeter	D	690	247	30
	E_t	1240	730	210
Lab. Uniaxial	E	304	199	98

the test results are shown in Table 8.10. For the uniaxial tests, a mean value of 199 MPa was obtained for the elasticity moduli, with a maximum of 304 MPa and a minimum of 98 MPa. For the uniaxial compressive strength a mean value of 1.4 MPa was obtained. The deformability moduli obtained using laboratory tests were generally lower than the values obtained with the in situ tests.

An overall analysis of the results for the different type of tests (plate load, pressuremeter and laboratory uniaxial tests) in the same type of rock mass, namely conglomerate of class C_L, was made. The results suggested that coefficients D and E_t decrease with the reduction in test volume. This is probably due to the fact that the tests were performed in locations with lower deformability coefficients which were chosen based on safety considerations (see Fig. 8.32). When the in situ PLTs were conducted on larger volumes, as with the 60 cm diameter rigid plate, the influence of more rigid blocks was more significant and the rock mass was observed to be stiffer. The comparative analysis of the results shows that the in situ plate tests with small diameters cannot represent behavior of the rock mass well. The mean deformability values obtained through large scale PLTs are closer to the real mean deformability value of the rock mass in the tested zone.

Figures 8.35 and 8.36 compare deformability coefficient D and tangential coefficient E_t. Figure 8.35 shows the values of the in situ deformability coefficients as: 30 cm plate load tests (D_{30}) against pressuremeter tests (D_d); 60 cm plate load tests (D_{60}) against pressuremeter tests; plate load tests D_{60} against plate load tests D_{30}. Using the least square method the following gradients were obtained: $D_{30} = 1.12D_d$; $D_{60} = 2.00D_d$; and $D_{60} = 1.61D_{30}$. Figure 8.36 compares tangential coefficients E_t. The relations were as follows: $E_{t30} = 1.12E_{td}$; $E_{t60} = 2.00E_{td}$; and $E_{t60} = 1.61E_{t30}$.

In conclusion, because of the heterogeneous nature of the rock mass, the deformability parameters are very much influenced by the dimension of the tested volumes and by the methodology followed. There is a significant difference in the deformability parameters that are obtained by PLTs of different diameters. This has real practical and important implications, specifically that if the PLT of diameter 30 cm results are used, then the Japanese regulations would not allow the dam to be constructed, whereas with the PLT of 60 cm results the permissions could be obtained to build the dam (Sousa et al. 1997).

Fig. 8.35 Comparison between in situ deformability coefficients
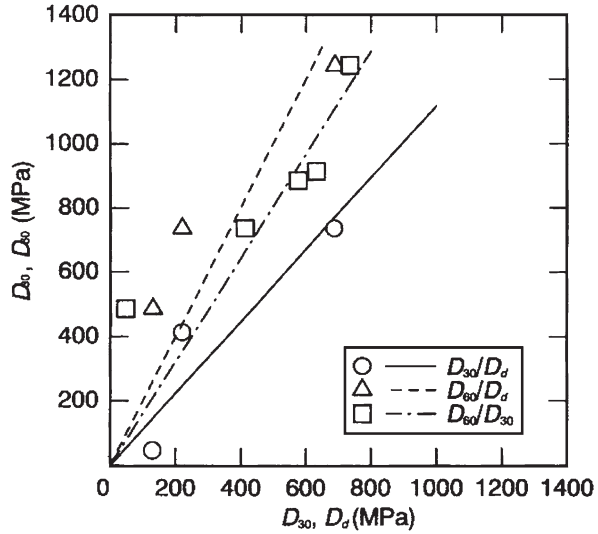
Fig. 8.36 Comparison between in situ tangential coefficients of elasticity E_t
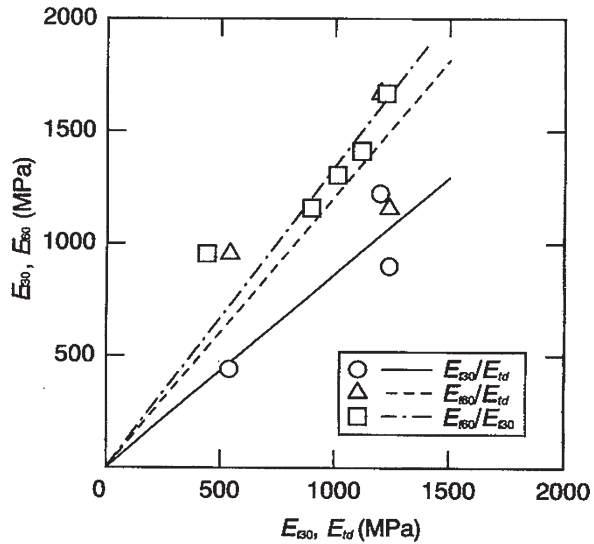
8.3 Methodology for Evaluating Strength

8.3.1 Strength Evaluation

Rock mass strength parameters can be determined using large scale in situ and laboratory tests for intact rock and discontinuities. The major in situ tests are sliding or shearing along discontinuities, in the fault filling materials and along other low strength surfaces and at rock mass/concrete interfaces. Laboratory tests for intact rock strength evaluation are shown in Table 8.4 (ASCE 1996; Rocha 2013).

In general, the unconfined compressive strength (UCS) of soft rocks varies between 2 and 20 MPa, and fiction angles normally range between 30° and 45° and cohesion values are typically not lower than 0.4 MPa (Rocha 1975). In addition, the shear strength of soft rock masses is less influenced by discontinuities than for hard rock, and the influence diminishes as the strength of the rock decreases. In the case of continuous fractures or continuous surfaces of low strength, each case should be considered individually as in the case of Água Vermelha presented in Sect. 8.1 (Rocha 1975; Pedro et al. 1975). There are cases where it is reasonable to adopt intact rock strength for the strength of the rock mass as was the case for Alto Rabagão dam, in Portugal, and for São Simão in Brazil (Rocha 1974).

Empirical systems provide good guidelines to estimate rock strength parameters for a given failure criterion. The GSI (Geological Strength Index) system was specifically developed to estimate rock mass strength parameters (Hoek 2007a). The system uses a qualitative description of two fundamental parameters of the rock mass: its structure, and the condition of its discontinuities. This system has also been used for evaluation of heterogeneous rock masses in the Porto Metro and tunnels in Greece that are in difficult rock mass conditions like flysch (Hoek et al. 2005; Babendererde et al. 2006).

Usually, the calculation of the GSI value is based on correlations with modified forms of the RMR and Q indices, taking into consideration the influence of groundwater and orientation of discontinuities (Hoek 2007a). Other approaches, defined by several authors, can be used for the GSI evaluation (Miranda 2003, 2007). Based on experimental data and theoretical fracture mechanics, the H-B criterion for rock masses is given by:

$$\sigma_1' = \sigma_3' + \sigma_c \left(m_b \frac{\sigma_3}{\sigma_c} + s \right)^a \tag{8.9}$$

where σ'_1 and σ'_3 are, respectively, the maximum and minimum effective principal stresses, m_b is a reduced value of the m_i parameter which is a constant of the intact rock, and s and a are parameters that depend on characteristics of the rock formation. Serrano and Olalla (2007) extended this failure criterion to 3D in order to consider the intermediate principal stress in the failure strength of rock masses.

The H-B criterion has seen developments introduced, as well as limitations (Douglas 2002; Carter et al. 2007; Carvalho et al. 2007). Once the value of GSI is determined, the parameters of the H-B criterion can be calculated through the following equations:

$$m_b = m_i \exp\left(\frac{GSI - 100}{28 - 14D} \right)$$

$$s = \exp\left(\frac{GSI - 100}{9 - 3D} \right) \tag{8.10}$$

$$a = \frac{1}{2} + \frac{1}{6}\left(\frac{GSI - 100}{9 - 3D}\right)$$

where D is a parameter developed for the underground works of the Porto Metro that depends on the disturbance to which the rock mass formation was subjected from blasting and stress relaxation (Hoek et al. 2002).

Guidelines were established for estimating D where $D = 0$ for excellent quality controlled blasting or excavations by TBMs and $D = 1$ for very large open pit mine slopes (Hoek 2007a). There is a drawback in this formulation since the excavation process affects a damaged zone near the excavation and it is not an intrinsic characteristic of the rock mass. As such it only represents the disturbed zone near the excavation. For GSI > 25, m_b can also be calculated through the expression:

$$m_b = m_i s^{\frac{1}{3}} \qquad (8.11)$$

For many cases of rock masses and for certain geotechnical software, it is convenient to use the equivalent cohesion c' and friction angle φ' to the H-B criterion. The range of stresses should be within $\sigma'_{1,RM} < \sigma_3 \leq \sigma'_{3RM}$. The value σ'_{3RM} can be determined for each specific case using.

$$\frac{\sigma'_{3\max}}{\sigma'_{cm}} = 0.47\left(\frac{\sigma'_{cm}}{\gamma H}\right)^{-0.94} \qquad (8.12)$$

For the shear strength of rock discontinuities the Q system can be used (Barton and Choubey 1977; Barton 2016). The failure criterion is expressed by:

$$\tau = \sigma_n \tan\left(JRC\, log_{10}\left(\frac{JCS}{\sigma_n}\right) + \varphi_r\right) \qquad (8.13)$$

where τ, σ_n, φ_r, JCS, and JRC are shear strength, normal stress, residual friction angle, joint compressive strength and joint roughness coefficient, respectively.

In the case of Bakhtiari dam site this empirical criterion was used with success for estimating the shear criteria of the discontinuities based on a statistical analysis (Sanei et al. 2015).

8.3.2   Use of Data Mining DM Techniques

Data Mining (DM) techniques have been used in many fields and recently in geotechnical engineering in different applications (Miranda 2007; Miranda and Sousa 2012; Sousa et al. 2012, 2017; Miranda et al. 2018). They are adequate as an advanced technique for analyzing large and complex databases with geotechnical

information within the framework of an overall process of Knowledge Discovery in Databases (KDD). KDD processes have been carried out in the context of rock mechanics using the geotechnical information of two hydroelectric schemes built in Portugal on mainly granite rock formations. The main goal was to find new models to evaluate strength and deformability parameters (namely friction angle, cohesion and deformability modulus) as well as the RMR index. Databases of geotechnical data were assembled and DM techniques were used to analyze and extract new and useful knowledge. The procedure allowed one to develop new, simple, and reliable models for geomechanical characterization of rock masses using different sets of input data, and which can be applied in different situations depending on availability of information (Miranda et al. 2009, 2011; Miranda and Sousa 2012).

With a database obtained from Venda Nova II hydroelectric scheme, the Mohr-Coulomb parameters derived from the H-B criterion were computed. For poorer rock mass conditions, the peak and residual parameters can be considered similar because a perfectly plastic post-peak behavior can be assumed. Prediction models for φ' and c' were developed. Figure 8.37 shows a plot of the most important parameters in the prediction of φ' (Miranda and Sousa 2012). There is a large number of variables that are significantly related to the prediction of φ' and several show similar importance. Having said this, the most important variables are: (1) UCS which is expected since it is a measure of strength; (2) the ratio between Jw/SFR; and (3) the Q index (with logarithmic transformation) as well as other variables related to the Q system. This was somewhat less expected because the Q system is normally used only for classification purposes and not for the calculation of strength parameters since it considers the rock mass as a continuum despite the Jr/Ja ratio being a strength index for joints. The Q index has shown to be complete and can be used for the prediction of geomechanical parameters. This was confirmed in Barton (2013).
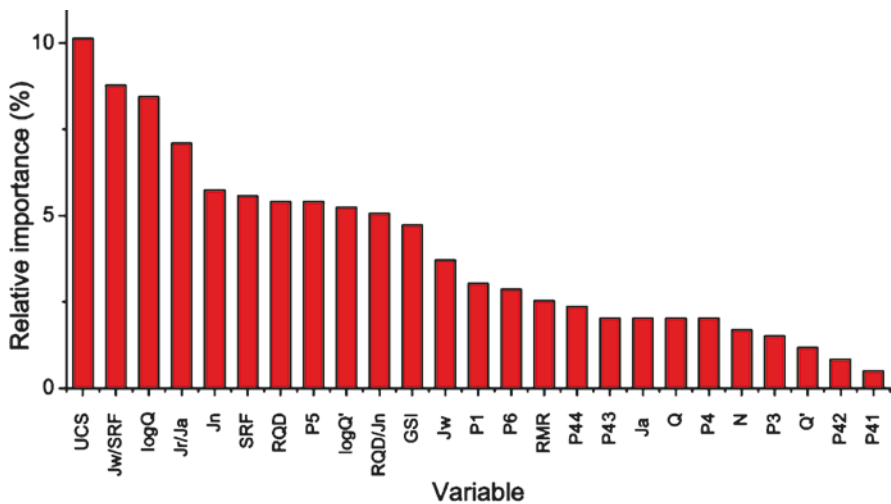

Fig. 8.37 Relative importance of the attributes for the prediction of friction angle (Miranda and Sousa 2012)

As an alternative classification system for the RMR system, the HRMR system has been developed. It adapts to the level of knowledge of the rock mass providing a classification with different accuracy levels, using a database including sound and very weathered granite formations. It is based on a large database of cases and has been validated in case studies. It allows one to visualize the surface and underground structures vividly (Miranda et al. 2014).

8.3.3 In Situ Shear Tests

Direct in situ shear tests can be conducted in discontinuities containing an infilling that has a critical influence on sliding stability. A typical set up of the direct shear equipment is shown in Fig. 8.38 (Wyllie 1999).

When studying dam sites, direct shear tests can be used on concrete-rock surfaces and special continuum surfaces with low strength such as in Água Vermelha dam (Rocha 2013).

In situ tests performed at LNEC for different dam sites studies were carried out as illustrated in Fig. 8.39, where a square-section of 70 cm was used (Rocha 2013). In order to obtain a more regular distribution of normal stresses, a shear force was applied by means of an inclined jack. The axes of the jacks pass through the center of the volume to be tested. This layout was advantageous for tests inside galleries. Once the vertical force was applied, which enabled the deformability of the rock

Legend:

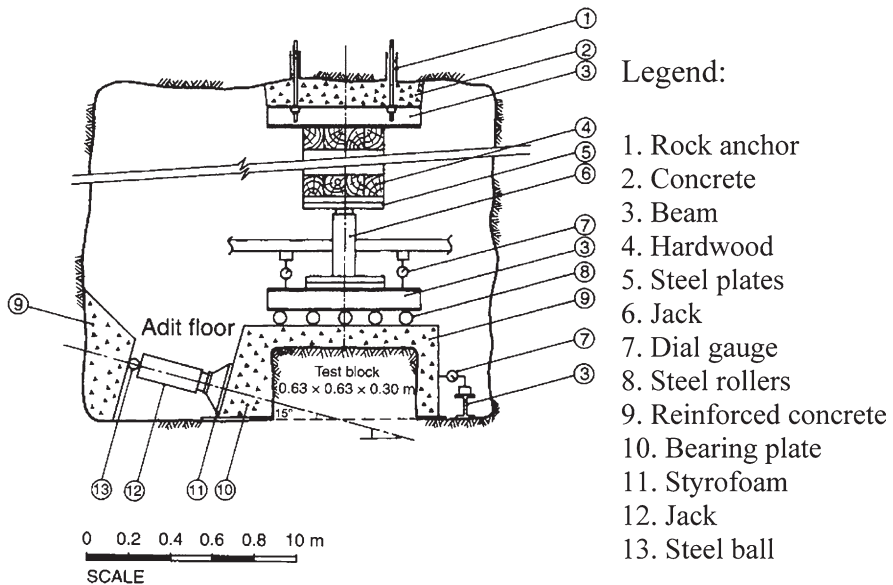1. Rock anchor
2. Concrete
3. Beam
4. Hardwood
5. Steel plates
6. Jack
7. Dial gauge
8. Steel rollers
9. Reinforced concrete
10. Bearing plate
11. Styrofoam
12. Jack
13. Steel ball

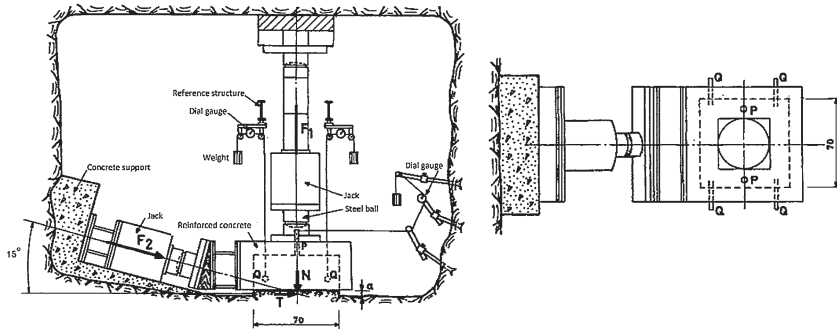**Fig. 8.38** Typical setup of an in situ shear test (Wyllie 1999)

**Fig. 8.39** In situ LNEC shear test (Rocha 2013)

Table 8.11 Shear strength of rocks tested in situ (adapted from Rocha 1964)

Rock formation	Type of test	Cohesion (MPa)	Friction angle (°)	Scheme	No. tests
Shale	Rock normal to schistosity	0.2	69	Bemposta (Portugal)	9
	Concrete-rock parallel to schistosity	0.2	60		5
	Concrete-rock parallel to discontinuities	0.2	63		3
Shale	Rock normal to schistosity	1.8	59	Valdecañas (Spain)	7
	Concrete-rock parallel to schistosity	0.4	62		3
Shale	Rock parallel to schistosity	0.4	59	Miranda (Portugal)	4
	Rock normal to schistosity	0.6	64		10
	Concrete-rock parallel to schistosity	0.4	62		8
	Concrete-rock normal to schistosity	0.7	60		8
Shale	Rock normal to schistosity	0.1	70	Alcantara (Spain)	16
	Concrete-rock parallel and normal to schistosity	0.1	56		28
Shale	Rock parallel to schistosity	0.2	50	Cambambe (Angola)	4
Sandstone	Rock parallel to schistosity	0.1	60	Cambambe (Angola)	4
	Concrete-rock parallel to schistosity	0.2	53		4

mass or of the discontinuity surface to be determined, the inclined force was applied by steps. Results of tests conducted by LNEC at several soft rock dam foundations are presented in Table 8.11. The rock are shale and sandstone, in dam sites in Portugal, Spain and Angola. Values of cohesion between 0.1 and 1.8 MPa were obtained, with an average of 0.4 MPa and friction angles between 53° and 70°, with an average of 60°.

Table 8.12 In situ shear tests on bedding planes at the Bakhtiari dam site (Sanei et al. 2015)

c_p (MPa)	φ_p (°)	φ_r (°)	JCS	JRC	σ_n (MPa)	τ_p (MPa)	τ_r (MPa)
0.36	31.9	31.7	27	6.4	1.05	0.94	0.93
0.31	34.6	34.5	20	8.7	1.55	1.33	1.31
0.10	33.0	32.3	26	7.1	0.89	0.60	0.59
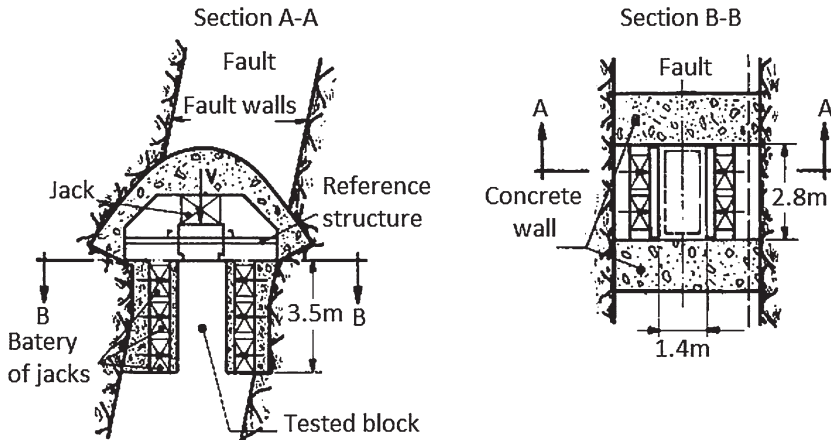
Fig. 8.40 Tests at Kurobe IV in Japan—large blocks were tested in this dam foundation (Rocha 2013)

In situ tests were recently performed at Bakhtiari dam site in Iran. This is the site of a hydroelectric power plant which includes the design and construction of a 315 m high, double curvature concrete dam and an underground powerhouse with a nominal output of 1500 MW (Sanei et al. 2015). Limestones layers constitute the foundation of the dam and of the powerhouse. In situ direct shear tests along rock discontinuities were performed. Three in situ tests on bedding planes were also performed on blocks with $70 \times 70 \times 35$ cm^3 in a gallery at Bakhtiari dam site. The rate of shear displacement ranged from 0.1 mm/min to 0.5 mm/min. The normal force was applied by hydraulic jacks and the shear force via a pressure plate. In the tests the normal stress varied from 0.59 to 7.03 MPa. The mechanical properties of the bedding planes obtained are given in Table 8.12, including cohesion and peak and residual friction angles. The parameters JCS and JRC of the Q system (Barton 2016) are also given as well as the applied pressures during tests (normal and peak and residual values).

In situ shear tests were performed at the Kurobe dam foundation site in Japan in basaltic formations (Rocha 2013). These tests were on a large scale, and are illustrated in Fig. 8.40. Tests were performed on a section of size 2.5×3.5 m^2. Tangential forces were successively applied in two perpendicular directions.

More recent equipment to determine the shear strength of rock masses in boreholes include the rock borehole shear test (RBST) apparatus, which is used in a
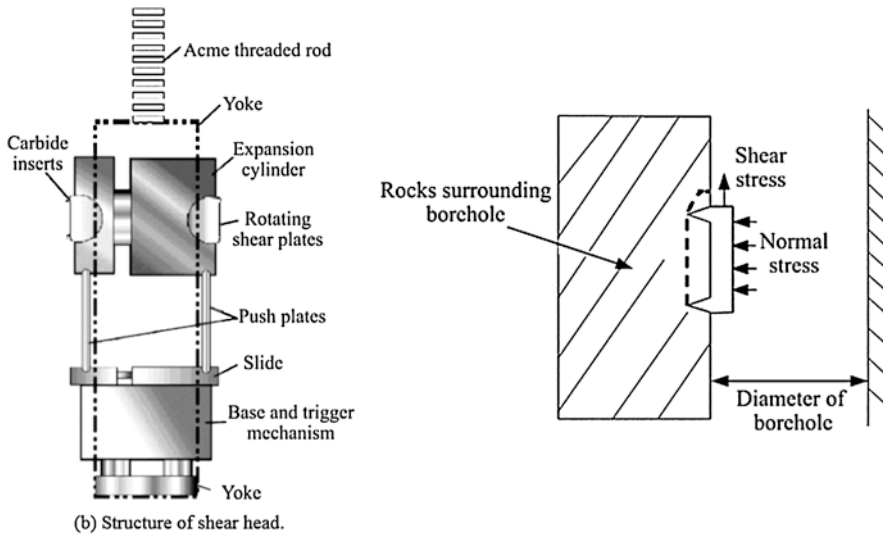
(b) Structure of shear head.

Fig. 8.41 Rock borehole shear tests (Yufei et al. 2012)

76 mm diameter borehole as shown in Fig. 8.41. This has found wide use in USA, Japan, Korea, and China (Zhao et al. 2012). This equipment was applied at the Xiangjiaba Hydropower Station which is one of the cascade power stations on the Jinsha River, in China. Due to the complicated geological conditions of the dam foundation, several groups of RBSTs tests were conducted on the black mudstone in the dam foundation. Forty three groups of shear strengths of black mudstone samples were obtained from RBSTs, and the shear strength parameters (c' and φ') were calculated. The average values of the internal friction coefficient and cohesion were 0.47 (about 25°) and 0.8 MPa, respectively.

8.3.4 Laboratory Tests of Discontinuities

It is common to determine the shear strength of discontinuities by using direct shear tests on core samples containing joint surfaces or bedding planes. Figure 8.42 presents a schematic shear box test with a rock sample under constant normal force (ASTM 2002). Shear tests are generally carried out with a constant normal force or stress. Dilatation can be inhibited by the surrounding rock mass and the initial normal stresses may increase with shear displacements. Different shear modes are illustrated in Fig. 8.43. In (a) and (c), the normal force is controlled, whereas in (b) and (d) the normal displacements are controlled.

Figure 8.44 shows the results of a test performed on a fractured basalt sample. It shows different types of behavior namely, tangential stresses vs. tangential displacements for different normal stresses; normal stresses vs. normal displacements; the
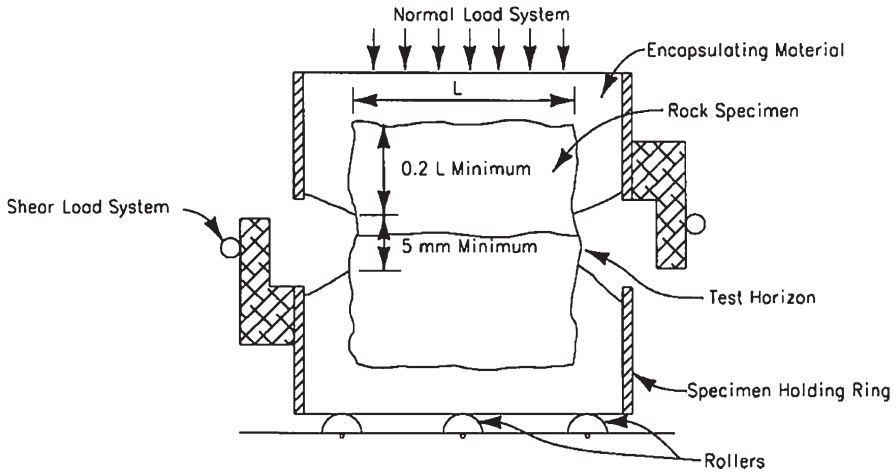
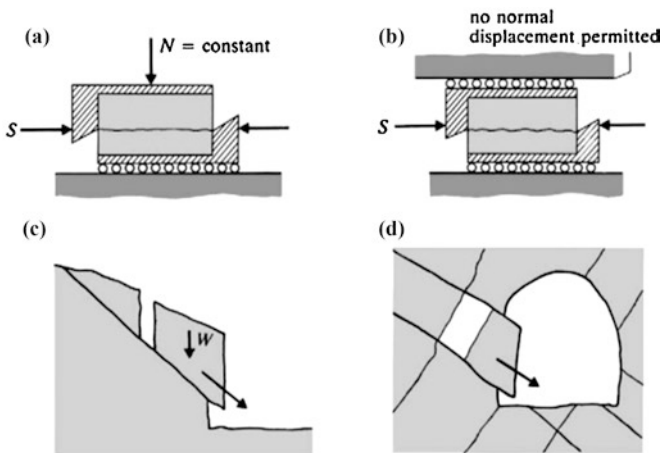**Fig. 8.42** Direct shear box with a specimen (ASTM 2002)

Fig. 8.43 Different situations of shear modes (Brady and Brown 2005)

dilatancy behavior of the discontinuity during the tests; and the peak and residual Coulomb criteria.

Other equipment has been developed by several laboratories and entities (Rocha 1974; Brady and Brown 2005; Wyllie and Mah 2010; Sanei et al. 2015). Figure 8.45 illustrates the classic equipment developed at LNEC (Rocha 2013). Figure 8.46 shows a special shear test developed at the University of Porto that allows one to conduct shear tests at normal stresses while allowing one to impose small deformations in the direction of the plane of the discontinuity. Figure 8.47 shows a portable device developed at the Imperial College that allows one to conduct tests in laboratory and in the field.

Fig. 8.44 Laboratory shear test results in a fractured basalt sample
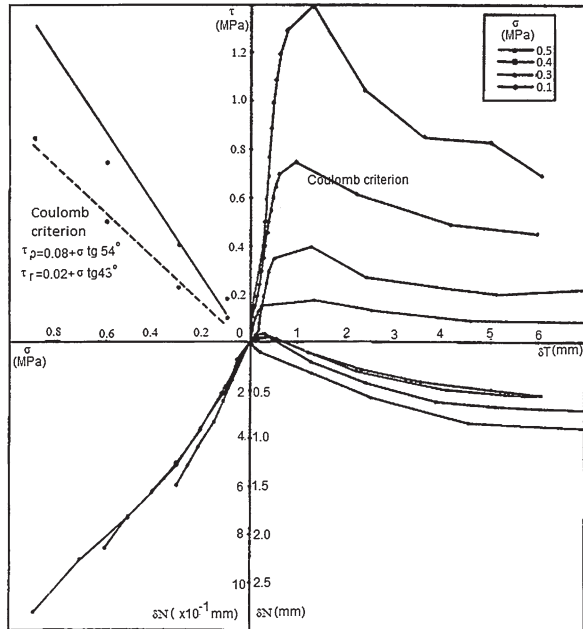
Fig. 8.45 Discontinuity shear tests at LNEC

Fig. 8.46 Discontinuity shear tests at University of Porto
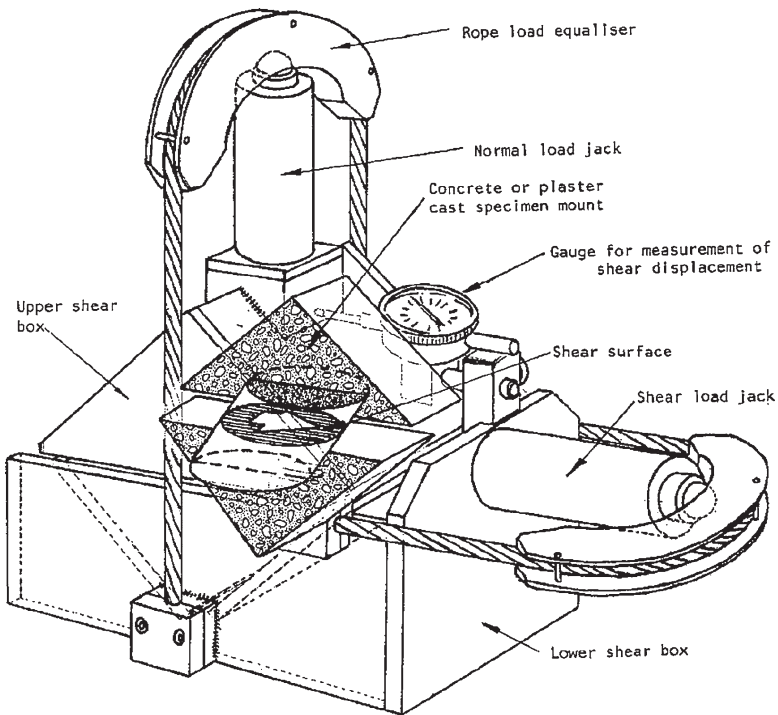
Fig. 8.47 Portable in situ test developed at Imperial College (Brady and Brown 2005)

Direct shear laboratory tests were performed on limestone samples from the Bakhtiari dam site in Iran (Sanei et al. 2015) which was discussed in the previous section. The purpose of these tests was to evaluate peak and residual shear strengths by applying normal and shear loads following the ISRM methods (Ulusay and Hudson 2007). The samples ranged from 5.4 to 14.8 cm in length in the direction of

Fig. 8.48 Peak friction angles of discontinuities in limestones (Sanei et al. 2015)

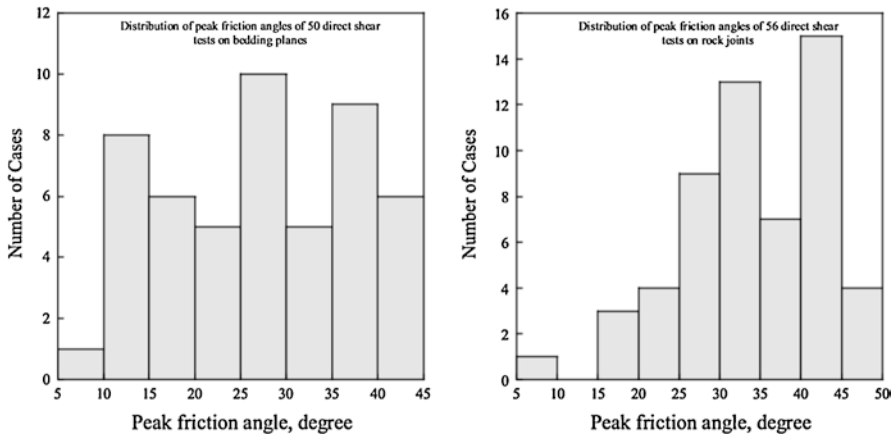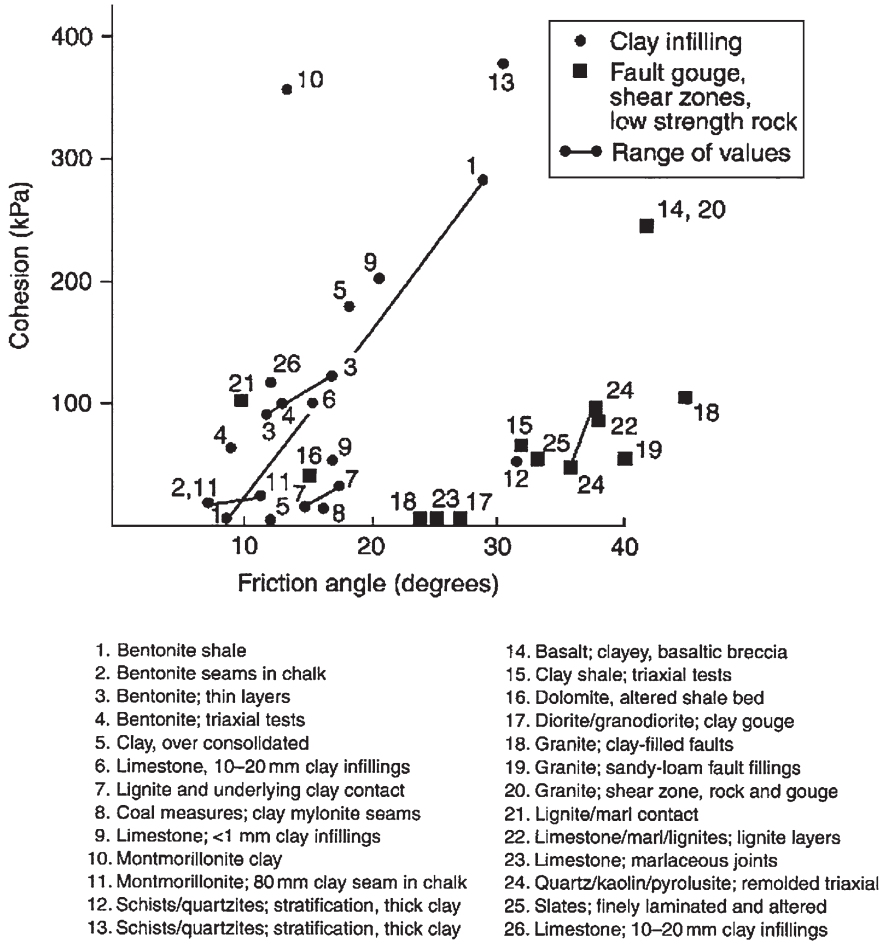shear. The normal stresses ranged between 0.47 and 3.2 MPa. The shear force was applied continuously while controlling the rate of shear displacement. In addition, the joint roughness coefficient JRC and joint compressive strength were evaluated. About 50 tests were conducted on bedding planes and 56 tests on rock joints. The distribution of peak and residual shear strengths are shown in Fig. 8.48.

In soft rocks, particularly weathered rocks, discontinuities are occupied with filling material. Consequently, strength of the joints is affected by the nature of the filling materials. Often, material like clay is present, and it is essential to investigate if these filler materials are continuous or if blocks are in direct contact (Rocha 1964; Wyllie and Mah 2010). Figure 8.49 shows the results of direct shear tests carried out in mainly soft rocks. These types of rocks are grouped depending on infilling materials (Wyllie and Mah 2010).

Other shear tests such as triaxial tests and torsion tests can be conducted. These are addressed in Wei et al. (2015). For the complete ISRM suggested methods for rock characterization and testing reference is made to Ulusay and Hudson (2007).

8.4 Conclusion

This chapter presents various methods to evaluate the geomechanical properties of rock masses, with emphasis on soft rocks. In general, there is a large degree of uncertainty associated with the evaluation of the deformability and strength properties of soft rock masses. The selection of appropriate values of these parameters requires a combination of in situ and laboratory tests as well as engineering judgment. The use of techniques based on artificial intelligence, particularly those based on Data Mining, have contributed to developing new geomechanical models for the evaluation and characterization of geomechanical properties of soft rock masses.

1. Bentonite shale
2. Bentonite seams in chalk
3. Bentonite; thin layers
4. Bentonite; triaxial tests
5. Clay, over consolidated
6. Limestone, 10–20 mm clay infillings
7. Lignite and underlying clay contact
8. Coal measures; clay mylonite seams
9. Limestone; <1 mm clay infillings
10. Montmorillonite clay
11. Montmorillonite; 80 mm clay seam in chalk
12. Schists/quartzites; stratification, thick clay
13. Schists/quartzites; stratification, thick clay

14. Basalt; clayey, basaltic breccia
15. Clay shale; triaxial tests
16. Dolomite, altered shale bed
17. Diorite/granodiorite; clay gouge
18. Granite; clay-filled faults
19. Granite; sandy-loam fault fillings
20. Granite; shear zone, rock and gouge
21. Lignite/marl contact
22. Limestone/marl/lignites; lignite layers
23. Limestone; marlaceous joints
24. Quartz/kaolin/pyrolusite; remolded triaxial
25. Slates; finely laminated and altered
26. Limestone; 10–20 mm clay infillings

Fig. 8.49 Shear strength of filled discontinuities (Wyllie and Mah 2010)

Common in situ and laboratory tests were described and the results of different tests were illustrated through several case studies. In general, refining predictions depends on better testing equipment, both in situ and in the laboratory, as well as the use of refined numerical models for interpretation. A case study of a dam in Japan with foundations on a heterogeneous conglomerate formation was described. In these formations, the geomechanical parameters are heavily influenced by the dimension of the tested volumes and of the methodology followed. The case illustrated that sometimes this can affect whether the construction of an engineering structure can proceed or not.

References

Alexeev AD, Revva VN, Molodetski AV (2013) Stress state effect on the mechanical behavior of coals under true triaxial compression conditions, chapter 21. In: Kwasniewski M, Li X, Takahashi M (eds) True triaxial testing of rocks. Taylor & Francis, London, pp 281–291

ASCE (1996) Rock foundations (technical engineering and design guides as adapted from US Army Corps of Engineers, no. 16). American Society of Civil Engineers, New York, p 129

ASTM (2002) Standard test method for performing laboratory direct shear strength test of rock specimens under constant normal force. ASTM D5607-02

Babendererde S, Hoek E, Marinos P, Cardoso S (2006) Characterization of granite and the underground construction in metro do Porto. In: Matos AC, Sousa LR, Kleberger J, Pinto PL (eds) Geotechnical risk in rock tunnels. Taylor & Francis, London, pp 41–51

Barton N (2000) TBM tunneling in jointed and faulted rock. Balkema, Rotterdam, p 172

Barton N (2013) Shear strength criteria for rock, rock joints, rockfill and rock masses: problems and some solutions. J. Rock Mech Geotech Eng 5(2013):249–261

Barton N (2016) Non-linear shear strength descriptions are still needed in petroleum geomechanics, despite 50 years of linearity. 50th US Rock Mechanics Symposium, ARMA Symposium, 16-252, Texas, p 14

Barton N, Choubey V (1977) The shear strength of rock joints in theory and practice. J Rock Mech 10:1–54

Bieniawski ZT (1989) Engineering rock mass classifications. Wiley, New York, p 251

Birid K (2014) Comparative study of rock mass deformation modulus using different approaches. 8th Asian Rock Mechanics Symposium, Sapporo, pp 553–563

Birid K (2015) Interpretation of pressuremeter tests in rocks. ISP7 Pressio Conference, pp 289–299

Brady B, Brown ET (2005) Rock mechanics in underground engineering. Kluwer Academic Publishers, New York, p 645

Carter T, Diederichs M, Carvalho J (2007) An unified procedure for Hoek-Brown prediction of strength and post yield behaviour for rock masses at the extreme ends of the rock competency scale. Proc. 11th ISRM Congress, Lisbon, pp 161–164

Carvalho J, Carter T, Diederichs M (2007) An approach for prediction of strength and post yield behaviour for rock masses of low intact strength. Proc. 1st Canada USA Rock Symposium, Vancouver, p 8

Castro AT, Sousa LR (1995) Interpretation of the monitored behavior of a large underground powerhouse using back-analysis techniques. Int. Conf. on engineering mechanics today, Hanoi

Douglas K (2002) The shear strength of rock masses. PhD Thesis, School of Civil and Environmental Engineering, University of New South Wales, Sydney, p 284

Failmezger R, Zdinak A, Darden J, Fahs R (2005) 50 years of pressiometers, vol 1. Press of ENPC/LCPC, Paris, pp 495–503

Fujii Y, Takahashi N, Takahashi T, Takemura T, Park H (2013) Fractographical analyses of the failure surfaces from triaxial extension tests on Kimachi sandstone, chapter 25. In: Kwasniewski M, Li X, Takahashi M (eds) True triaxial testing of rocks. Taylor & Francis, London, pp 323–329

Graça JC (1983) Deformability – BHD method. In: Recent developments in rock mechanics. LNEC, Lisbon, pp 29–58 (in Portuguese)

Grossmann N (1993) New developments in the in-situ determination of rock mass parameters. Course on dam foundations in rock masses. LNEC, Lisbon

He M (2006) Rockburst disasters in coal mine. Glob Geol 9(2):121–123

He M (2014) Latest progress of soft rock mechanics and engineering in China. J Rock Mech Geotech Eng 6:165–179

He M, Sousa LR (2014) Experiments on rock burst and its control. AusRock 2014: Third Australasian ground control in mining conference, Sydney, pp 19–31

He M, Jia XN, Gong W, Liu G, Zhao F (2013) A modified true triaxial test system that allows a specimen to be unloaded on one surface, chapter 19. In: Kwasniewski M, Li X, Takahashi M (eds) True triaxial testing of rocks. Taylor & Francis, London, pp 251–266

He M, Sousa LR, Miranda T, Zhu G (2015a) Rockburst laboratory tests database: application of data mining techniques. J Eng Geol Geol Geotech Hazard 185(2015):116–130

He M, Sousa RL, Muller A, Vargas JRE, Sousa LR, Chen X (2015b) Analysis of excessive deformations in tunnels for safety evaluation. J Tunnel Undergr Space Technol 45(2015):190–202

Hoek E (2007a) Practical rock engineering. www.rocscience.com

Hoek E (2007b) Big trends in bad rock. Therzaghi lecture. ASCE J Geotech Geoenviron Eng 127(9):726–740

Hoek E, Marinos P (2009) Tunneling in overstressed rock. Symp. EUROCK 2009, Dabrovnik, p 13

Hoek E, Carranza-Torres C, Corkum B (2002) The Hoek-Brown failure criterion – 2002 edition. Proc. 5th north American rock mechanics Sym. And 17th tunneling Assn of Canada conf. NARMS-TAC, Toronto, pp 267–271

Hoek E, Marinos PG, Marinos VP (2005) Characterization and engineering properties of tectonically undisturbed but lithologically varied sedimentary rock masses. Int J Rock Mech Min Sci 42(2005):277–285

Hoek E, Torres C, Diederichs M, Corkum B (2008) Integration of geotechnical and structural design in tunneling. 56th Annual geotechnical engineering conference, Minneapolis, p 53

Kanji MA (2014) Critical issues in soft rocks. J Rock Mech Geotech Eng 6:186–195

Kwasniewski M (2013) Mechanical behavior of rocks under true triaxial compression conditions – a review, chapter 8. In: Kwasniewski M, Li X, Takahashi M (eds) True triaxial testing of rocks. Taylor & Francis, London, pp 99–138

Kwasniewski M, Li X, Takahashi M (2013) True triaxial testing of rocks. CRC Press, Taylor & Francis Group, London, p 367

Lade PV (2013) Estimating the parameters for a three-dimensional failure criterion for rocks from a single test, chapter 15. In: Kwasniewski M, Li X, Takahashi M (eds) True triaxial testing of rocks. Taylor & Francis, London, pp 213–222

Li X, Shi L, Bai B, Li Q, Xu D, Feng X (2011) True-triaxial techniques for rocks – state of the art and future perspectives, chapter 1. In: Kwasniewski M, Li X, Takahashi M (eds) True triaxial testing of rocks. Taylor & Francis, London, pp 3–18

Lu Y, Chen M, Jin Y, Yang P, Yuan J, Fan K (2012) Experimental study of wellbore deformation in a deep claystone formation, chapter 22. In: Kwasniewski M, Li X, Takahashi M (eds) True triaxial testing of rocks. Taylor & Francis, London, pp 293–300

Martins CS, Sousa LR (1989) Recent advances in the interpretation of the small flat jack method. ISRM Congress, Montreal

Medley EW (1994) Engineering characterization of melanges and similar block-in-matrix rocks (bimrocks). PhD thesis, Department of Civil Engineering, University of California at Berkley

Miranda T (2003) Contribution to obtaining geomechanical parameters for the modeling of underground works in granite rock masses. MSc Thesis, University of Minho, Guimarães, p 186 (in Portuguese)

Miranda T (2007) Geomechanical parameters evaluation in underground structures. Artificial Intelligence, Bayesian probabilities and inverse methods. PhD Thesis, University of Minho, Guimarães, p 291

Miranda T, Sousa LR (2012) Application of data mining techniques for the development of geomechanical characterization models for rock masses. In: Sousa LR, Vargas E, Fernandes MM, Azevedo R (eds) Innovative numerical modeling in geomechanics. Taylor & Francis, London, pp 245–264

Miranda T, Correia AG, Sousa LR (2009) Bayesian methodology for updating geomechanical parameters and uncertainty quantification. Int J Rock Mech Min Sci 46(7):1144–1153

Miranda T, Sousa LR, Correia A (2011) Development of models for geomechanical characterization using Data Mining techniques applied to a database gathered in underground structures. 45th US Rock Mechanics Symposium, San Francisco, 10 in CD-ROM

Miranda T, Sousa LR, Tinoco J (2014) Updating of the hierarchical rock mass rating (HRMR) system and a new subsystem developed for weathered granite formations. J Min Sci Technol 24:769–775

Miranda T, Sousa LR, Gomes AT, Tinoco J, Ferreira C (2018) Volcanic rocks geomechanical characterization by using empiric systems. J Rock Mech Geotech Eng 10:138–150

Mogi K (2013) How I developed a true triaxial rock testing machine, chapter 9. In: Kwasniewski M, Li X, Takahashi M (eds) True triaxial testing of rocks. Taylor & Francis, London, pp 139–157

Pacheco F, Caxito F, Moraes L, Marangoni Y, Santos R, Soares A (2017) Basaltic ring structures of the Serra Geral formation at the southern region, Triângulo Mineiro, Água Verrmelha region, Brazil. J Volcanol Geotherm Res 355:136–148

Palmstrom A, Singh R (2001) The deformation modulus of rock masses – comparisons between in-situ tests and indirect estimates. J Tunnel Undergr Space Technol 16(3):115–131

Pedro JO, Sousa LR, Teles M, Ramos JM (1975) Study of the Água Vermelha dam by the finite element method. LNEC Report, Lisbon (in Portuguese)

Pinto JL (1981) Determination of the deformability modulus of weak rock masses by means of large flat jacks (LFJ). ISRM Symp. on weak rocks, Tokyo

Pinto JL (1983) Deformability – LFJ method. In: Recent developments in rock mechanics. LNEC, Lisbon, pp 3–27 (in Portuguese)

Pinto JL, Graça C (1983) State of stress – SFJ method. In: Recent developments in rock mechanics. LNEC, Lisbon, pp 41–58 (in Portuguese)

River Bureau (1986) Manual for river works in Japan. Design of dams. Ministry of Construction, Tokyo

Rocha M (1964) Mechanical behavior of rock foundations in concrete dams. Proc 8th Congress on large dams, Edinburgh, vol 1, pp 785–831

Rocha M (1974) Present possibilities of studying foundations of concrete dams. 3rd ISRM Congress, Denver, pp 879–897

Rocha M (1975) Some problems regarding rock mechanics of low strength materials. V Pan-American Congress on Soil Mechanics and Foundation Engineering, Buenos Aires, pp 489–514 (in Portuguese)

Rocha M (1978) Analysis and design of the foundation of concrete dams. ISRM Symp. on rock mechanics applied to dam foundations, Rio de Janeiro, vol 3, pp 3.11–3.70

Rocha M (2013) Rock mechanics, special edn. LNEC, Lisbon, p 445 (in Portuguese)

Rodrigues FP, Graça JC (1983) Heterogeneity. In: Recent developments in rock mechanics. LNEC, Lisbon, pp 123–159 (in Portuguese)

Rodrigues FP, Grossman NF, Rodrigues LF (1978) Rock mechanics tests of the Mingtan pumped storage project. LNEC Report, Lisbon, 2 Vol

Sanei M, Faramarzi L, Fahimifar A, Goli S, Mehinrad A, Rahmati A (2015) Shear strength of discontinuities in sedimentary rock masses based on direct shear tests. Int J Rock Mech Min Sci 75(2015):119–131

Serrano A, Olalla C (2007) Bearing capacity of shallow and deep foundations in rock with the Hoek and Brown failure criteria. Proc. 11th ISRM Congress, Lisbon, vol 3, pp 1379–1392

Simon R, Deng D (2009) Estimation of scale effects in intact rock using dilatometer tests results. Geohalifax2009, pp 481–488

Slope Indicator (2010) Goodman jack. Slope Indicator, Washington, DC, p 23

SolExperts (2016) Dilatometer measurements. Brochure. SolExperts, Monchaltorf, p 2

Sousa LR (2006) Learning with accidents and damage associated to underground works. In: Matos AC, Sousa LR, Kleberger J, Pinto PL (eds) Geotechnical risks in rock tunnels. Taylor & Francis, London, pp 7–39

Sousa RL (2010) Risk analysis for tunneling projects. PhD Thesis, MIT, Cambridge, p 589

Sousa RL, Einstein H (2012) Risk analysis during tunnel construction using Bayesian networks: Porto metro case study. Tunnel Undergr Space Technol 27(2012):86–100

Sousa LR, Nakamura A, Yoshida H, Yamaguchi Y, Kawasaki M, Satoh H (1997) Evaluation of the deformability of rock masses for dam foundations. Analysis of deformability investigation results of heterogeneous bedrock. Technical Memorandum of PWRI, no. 3514, Tsukuba City, 45p

Sousa LR, Chapman D, Miranda T (2010) Deep rock foundations of skyscrapers. J Soils Rocks 33(1):3–22

Sousa LR, Miranda T, Roggenthen W, Sousa RL (2012) Models for geomechanical characterization of the rock mass formations at DUSEL using data mining techniques, US Rock Mechanics Symposium, Chicago, 14p (CD-ROM)

Sousa LR, Wang X, Guo Q, Dias D, Yuan P, Sousa RL (2015) Stability and risk analysis of ancient cavities in historical areas. The case of Yulin caves. China Int Symp on Scientific problems and long-term preservation of large-scale ancient underground engineering, Longyou, pp 411–418

Sousa LR, Miranda T, Sousa RL, Tinoco J (2017) The use of data mining techniques in rockburst assessment. J Eng 3(2017):552–558

Tarasov B (2012) Superbrittle failure regime of rocks at conventional triaxial compression, chapter 27. In: Kwasniewski M, Li X, Takahashi M (eds) True triaxial testing of rocks. Taylor & Francis, London, pp 343–350

Tshibangu JP, Descamps F (2013) The FPMs (UMons-Belgium) device for investigating the mechanical behavior of materials subjected to true triaxial compression, chapter 4. In: Kwasniewski M, Li X, Takahashi M (eds) True triaxial testing of rocks. Taylor & Francis, London, pp 51–60

Ulusay R, Hudson J (2007) The complete ISRM suggested method for rock characterization, testing and monitoring: 1974–2006. ISRM Turkish National Group, Ankara, Turkey, p 613

Wei Y, Fu W, Nie D (2015) Nonlinearity of rock joint shear strength. Strength Mater 47(1):205–212

Wyllie D (1999) Foundations on rock. E & FN Spon, London, p 401

Wyllie D, Mah CW (2010) Rock slope engineering. Taylor & Francis, London, p 431

Yufei Z, Wang X, Zhang X, Jia Z, Zeng X, Zhang H (2012) Rock borehole shear tests in dam foundation of Xiangjiaba hydropower station. J Rock Mech Geotech Eng 4(4):360–366

Yufin S, Lamonina E, Postolskaya O (2007) Estimating of strength and deformation parameters of jointed rock masses. 5th Int. Work. on applications of computational mechanics in geotechnical engineering, Guimarães, pp 3–15

Zhao Y, Wang XG, Zhang XH, Jia Z, Zeng X, Zhang H (2012) Rock borehole shear tests in dam foundation of Xiangjiaba hydropower station. J Rock Mech Geotech Eng 4(4):360–366

Zhou C (2018) Study and development of sample preparation and triaxial test equipment for soft rocks. Report. Zhongshan University, Guangzhou, p 37